St. John's University
St. John's Scholar

Theses and Dissertations

2021

CHARACTERIZING FERROPTOSIS PATHWAYS IN IN VITRO MOTOR NEURON MODELS

Alejandra Martinez
Saint John's University, Jamaica New York

Follow this and additional works at: https://scholar.stjohns.edu/theses_dissertations

Part of the Biology Commons, and the Cell Biology Commons

Recommended Citation

Martinez, Alejandra, "CHARACTERIZING FERROPTOSIS PATHWAYS IN IN VITRO MOTOR NEURON MODELS" (2021). *Theses and Dissertations*. 227.
https://scholar.stjohns.edu/theses_dissertations/227

This Dissertation is brought to you for free and open access by St. John's Scholar. It has been accepted for inclusion in Theses and Dissertations by an authorized administrator of St. John's Scholar. For more information, please contact fazzinol@stjohns.edu.

CHARACTERIZING FERROPTOSIS PATHWAYS IN IN VITRO MOTOR NEURON MODELS

A dissertation submitted in partial fulfillment
of the requirements for the degree of

DOCTOR OF PHILOSOPHY

to the faculty of the

DEPARTMENT OF BIOLOGICAL SCIENCES

of

ST. JOHN'S COLLEGE OF LIBERAL ARTS AND SCIENCES

at

ST. JOHN'S UNIVERSITY
New York
by
Alejandra Martinez

Date Submitted 3/18/2021 Date Approved 5/24/2021

Alejandra Martinez Dr. Wan Yang

© Copyright by Alejandra Martinez 2021

All Rights Reserved

ABSTRACT

CHARACTERIZING FERROPTOSIS PATHWAYS IN IN VITRO MOTOR NEURON MODELS

Alejandra Martinez

Ferroptosis is a non-apoptotic regulated form of cell death driven by the toxic accumulation of lipid peroxides and the presence of iron. The mechanism by which ferroptosis operates requires further investigation; here I will discuss the findings regarding the role of ferroptosis in different cellular models as well as the genes that may be involved with either promoting or hindering the ferroptotic pathway. NSC-34 is a hybrid cell line of neuroblastoma and primary spinal cord cells that can be differentiated into a motor neuron-like state allowing the characterization of ferroptosis in two distinct cellular conditions. Additionally, iNIL cells are a mouse embryonic stem cell line that can be efficiently differentiated into motor neurons and provides a viable cellular model to study ferroptosis in neuronal context. Contrarily, HT-1080 is the mother cell line in which ferroptosis was discovered, providing the best model to look at which genes are essential to drive ferroptosis. PPIP5K2 is a gene involved in phosphate homeostasis that, upon knockdown via siRNA transfection, showed rescue of cell death after ferroptosis induction. ACSL4 is another gene of interest since it is involved in lipid metabolism and lethal accumulation of lipid ROS is a hallmark of ferroptosis. Thus, generating stable cell lines with knockouts of such genes via lentiviral CRISPR transduction in both HT-1080 and mouse embryonic stem cells are essential to establish further connections.

ACKNOWLEDGEMENTS

Thank you to my parents who inspired my love for science and encouraged my inquisitive nature from a very young age.

Thank you to my mentor Dr. Wan Yang, who supported me and encouraged me to overcome hurdles; I had the opportunity to learn so much in regard to scientific phenomena as well as the critical thinking that is imperative in research, above all I learned the type of scientist I want to be. Thank you to my committee members Dr. Matteo Ruggiu, Dr. Ivana Vancurova, Dr. Yong You, and Dr. Yan Zhu for your support. Thank you to all of the faculty in the Department of Biological Sciences. Thank you to all lab members who assisted in carrying out this research: Fahmida Patwari, Jovan Mirkovic and Zofia Stanisz who helped with the NSC-34 work; Aashna Meghjani, Ahryun Kim and Cristina Aguilar who helped with the iNIL work; Mohammed Shah who helped with the CRISPR work; and current lab member Jay Katragadda.

Thank you to our collaborators Esteban Mazzoni, Barbara Corneo, and Andreas Hermann.

TABLE OF CONTENTS

ACKNOWLEDGEMENTS ii
LIST OF FIGURES v
CHAPTER 1: INTRODUCTION 1
CHAPTER 2: MATERIALS AND METHODS 6
Cell Culture 6
NSC-34 6
iNIL 6
iNIL Cells Differentiated into Motor Neurons 7
HT-1080/HT-1080 gALOX5 9
HEK-293T 9
Chemicals and Antibodies 9
Inducing Ferroptosis in NSC-34 Cells 10
Inducing Ferroptosis in iNIL MNs 11
Inducing Ferroptosis in HT-1080 12
Resazurin Viability Assay 12
Light Microscopy 13
Analysis of Lipid Reactive Oxygen Species Generation 13
Gene Expression Analysis by RT-qPCR 14
Measuring HB9/GFP Expression in iNIL Cells 15
Immunostaining iNIL Cells 15
siRNA Transfection 16
CRISPR Molecular Cloning 17
Designing Oligos 18
PolyJet Transfection/Lentivirus Production 18
CRISPR Knockout HT-1080 19
CRISPR Knockout iNIL 20
Blasticidin Selection 20
CHAPTER 3: RESULTS 22
NSC-34 Cells Are Sensitized to Ferroptosis Upon Differentiation 22
Embryonic Stem Cells Differentiated into MNs Are Sensitized to Ferroptosis 33
PPIP5K2 Knockdown Inhibits Cell Death Induced by Ferroptosis 42

CRISPR Knockouts Provide Stable Cell Lines for Genetic Studies in HT-1080..... 45
ACSL4 Presents as a Potential Genetic Target in Ferroptosis..... 50
CRISPR Knockout Optimized for Embryonic Stem Cell Stable Cell Lines 52
iNIL MN Ferroptosis Model Reveals Competency of ALS Drugs 53
CHAPTER 4: DISCUSSION..... 56
NSC-34 Provides a Basis for Studying Ferroptosis in a MN Context..... 56
Embryonic Stem Cells Provide a Better Model for Studying Ferroptosis Sensitivity in MNs..... 58
Why are Motor Neurons Sensitive to Ferroptosis?..... 61
The Importance of Genetic Studies in Understanding Ferroptosis in Future Experiments 62
iNIL Cells Differentiated into MNs Provide a Viable Model to Screen ALS drugs 63
and Find Potential Therapeutic Targets for Neurodegenerative Pathologies 63
REFERENCES 64

LIST OF FIGURES

Figure 1: Ferroptosis induction in NSC-34 cell line with erastin and RSL3 23
Figure 2: Optimal condition to induce ferroptosis in NSC-34..... 24
Figure 3: Cell death induced by FINs is ferroptosis specific..... 26
Figure 4: Optimal condition to differentiate NSC-34 into a motor neuron-like state..... 27
Figure 5: NSC-34 differentiated cells are more sensitive to cell death 29
Figure 6: Extrinsic factors involved in NSC-34 sensitivity differences 30
Figure 7: Intrinsic factors involved in NSC-34 sensitivity differences 31
Figure 8: iNIL mouse embryonic stem cells are differentiated into MNs 34
Figure 9: MNs are sensitized to ferroptosis via RSL3 induction..... 37
Figure 10: IPA analysis reveals pathways involved in MN sensitivity to ferroptosis..... 39
Figure 11: Downregulation of calcium signaling pathway drives ferroptosis in MN context..... 40
Figure 12: IPA Analysis suggests upstream regulator of downregulated genes..... 41
Figure 13: siRNA knockdown of PPIP5K2 inhibits ferroptosis..... 44
Figure 14: CRISPR knockout in HT-1080 cell line..... 47
Figure 15: CRISPR is used to overexpress gfp in HT-1080..... 49
Figure 16: CRISPR knockout of ACSL4 in HT-1080 inhibits ferroptosis..... 52
Figure 17: CRISPR is used to overexpress gfp in iNIL cells 53
Figure 18: ALS drug edaravone inhibits ferroptosis in this MN model 55

CHAPTER 1: INTRODUCTION

Cell death modalities are increasingly investigated for their potential roles in various disease contexts, from cancer to neurodegeneration. Apoptosis is among the more well-established pathways. However, other cell death modalities such as ferroptosis and necroptosis are regulated non-apoptotic forms of cell death that require further characterization. While both are imperative in understanding their impact on cellular function and the possible roles they play in a pathological context, ferroptosis was the main focus of this study. This particular cell death pathway has yet to be fully characterized, lacking information on specific key regulators that facilitate it as well as its function and importance in varying cell models.

Ferroptosis differs from other modes of cell death because it lacks the swelling of the cytoplasm and rupture of the cell membrane typical to necrosis[1]. It does not embody the morphological characteristics of apoptosis that include cell shrinkage, chromatin condensation, formation of apoptotic bodies and disintegration of the cytoskeleton[1]. While the formation of classical closed bilayer membrane structures such as autophagic vacuoles are the epitome of autophagy, this too is a feature uncommon in ferroptosis[1]. Ferroptosis manifests morphologically with an increased membrane density and shrinkage of the mitochondria[1]. Its most notable hallmarks are the production of cytosolic and lipid reactive oxygen species (ROS) as a result of metabolic dysfunction but independent of the mitochondria[1]. This accumulation of ROS to lethal amounts is iron dependent. The role of iron in catalyzing ferroptosis remains elusive yet crucial in driving cellular death either via Fenton chemistry or through enzymatic processes.

Glutathione peroxidase 4 (GPX4) is an enzyme containing eight nucleophilic amino acids, including seven cysteines and one selenocysteine enabling it to react with electrophiles in the cell[2,3]. Under normal physiological conditions, GPX4 is a key antioxidant in regulating oxidative stress by reducing toxic lipid peroxides to non-toxic lipid alcohols in the presence of its cofactor glutathione (GSH)[2]. GSH is a tripeptide composed of the three amino acids cysteine, glutamic acid, and glycine. Its antioxidant properties play a major role in maintaining cellular health since it serves as a scavenger of free radicals. If otherwise left unchecked, these free radicals have the potential to dismantle the cell. On the other hand, GSH also serves as a co-enzyme for GPX4, entering an oxidized state as GPX4 catalyzes the reduction of ROS. GSH can then be recycled by glutathione reductase and the duo can continue to minimize oxidative stress.

During ferroptosis there are two major events that must occur to carry out the process; the first is an inhibition of the reduction of lipid peroxides. This inhibition transpires when GPX4 and GSH function is compromised. The second event is the formation of lipid peroxides which materializes via three distinct routes all of which are iron dependent: lipid ROS produced through the Fenton reaction by iron in a non-enzymatic manner, lipid peroxides produced by lipid autoxidation in an iron-catalyzed manner and lipid peroxides generated by oxygenation and esterification of polyunsaturated fatty acids (PUFAs)[2,3]. Whether any of these routes to generate lipid ROS is predominant in the ferroptotic pathway is still under investigation. In any case, the two major events promote an increase in lipid ROS to lethal amounts and highlight the importance of GPX4 and GSH; two main targets for many small molecules to induce ferroptosis.

Erastin and RSL3 are the two canonical drug inducers of ferroptosis via inhibition of system Xc and GPX4, respectively. These small molecules were the first ferroptosis-inducing compounds discovered using high-throughput screening of small molecule libraries[4,5]. They were found to promote a type of cell death in conditions where both apoptosis and necroptosis hallmarks were repressed[6]. In the case of apoptosis this included caspases, BAX, and BAK; while for necroptosis both RIPK1 and RIPK3 were targeted[6]. Since these results deviated from the norm, it inspired further research and both erastin and RSL3 are now exceptionally well understood.

Erastin blocks the system Xc antiporter, preventing the import of cystine and export of glutamate at a 1:1 ratio. Cystine is a dimer that can be reduced to cysteine in the cell and subsequently is vital to the production of glutathione. Thus, erastin's mechanism of action to induce ferroptosis is to indirectly inhibit GPX4 by depleting glutathione[6]. On the other hand, RSL3 directly inhibits GPX4's enzyme function leading to an increase in lipid ROS and eventual cell death[6]. These small molecules are efficient ferroptotic inducers that can be manipulated to study the pathway in detail within several cellular models including but not limited to NSC-34 and mouse embryonic stem cells.

The NSC-34 cell line is a hybrid cell line developed by fusing the aminopterin-sensitive neuroblastoma N18TG2 with motor neuron (MN) enriched embryonic day 12-14 spinal cord cells[7]. These cells were developed with the anticipation to create a neuronal immortal clonally uniform cell line. Its development would be a great feat in overcoming some of the setbacks when investigating motor neurons. For instance, this cell line is easily cultured and survives several passages. Meanwhile other motor neuron differentiation processes require complex media and weeks before any experimentation

can commence. Interestingly, these cells also embody several motor neuron properties when differentiated, including the following: development of long processes and S-laminin with leucine-arginine-glutamate (LRE) adhesion motif, the formation of contacts with myotubes in culture and increased survival in the presence of neurotrophic factors.[7,8] Overcoming these hurdles and providing a system to investigate motor neurons harboring several of its key features led to the use of NSC-34 in the study.

iNIL cells are a mouse embryonic stem cell line generated by the Mazzoni lab also providing an efficient experimental motor neuron model.[9] The development of this cell line takes advantage of the recent progress in programming cell fate by transcription factors, receiving the name iNIL as a result of the three transcription factors Neurogenin 2, Insulin gene enhancer protein and LIM Homeobox 3.[9] Intriguingly, there are two proposed models suggested for how programming modules regulate cellular identity: the independent model and the synergistic model.[9] The former hypothesizes that each transcription factor works independently to determine cell fate: binding to distinct genetic locations. The latter suggests the transcription factors jointly bind to common regulatory elements to work in tandem to promote the specific cell fate.[9]

Upon investigation it was determined that Isl1 and Lhx3 directly interact forming a heterodimer that synergistically regulate cell fate.[9] Contrarily, individual mutations in Isl1 and Lhx3 effects the ultimate phenotype indicating the individual model may still be involved.[9] Although the specific model for how transcription factors program cells could not be elucidated, the definitive differentiation of iNIL cells into MNs using these transcription factors was well established in the study.[9] Researchers developed this embryonic stem cell line with NIL factors to be doxycycline inducible allowing for

biochemical analysis and validation of successful differentiation.[9] Not only were these cells effectively differentiated into spinal MNs but the same process could be induced using sonic hedgehog and retinoid acid the two patterning signals involved in the normal process of MN development.[9] Along with NSC-34, iNIL was a useful MN model to investigate ferroptosis in this study.

CHAPTER 2: MATERIALS AND METHODS

Cell Culture

NSC-34

NSC-34 cells were purchased from Cedarlane (Burlington, NC, USA) (cat. no. CLU140). Cells under normal conditions were grown in DMEM 10% FBS with penicillin and streptomycin antibiotics (pen/strep). NSC-34 cells were differentiated after harvesting using trypsin/EDTA and washing the cell pellet twice with the corresponding differentiation medium before seeding into collagen coated culture plates (Corning BioCoat, Corning, NY, USA; cat. no. 354400). The following were the four differentiation conditions: (a) 'MEM' – minimum essential medium a (Thermo Fisher Scientific, Waltham, MA, USA; cat. no. 12571063), (b) 'MEM with atRA' – MEM with 1uM all-trans-retinoic acid (Sigma-Aldrich, St Louis, MO, USA; cat. no. R2625), (c) 'F12' – 1:1 of DMEM and Ham's F12 (Corning Cellgro cat. no. 10-090-CV), and (d) 'F12 with atRA' – F12 medium with 1uM all-trans-retinoic acid. All differentiation media were supplemented with 1% FBS, nonessential amino acids (Thermo Fisher Scientific, cat. no. 11140050), and pen/strep.

iNIL

iNIL cells are thawed and re-suspended in feeder media. Feeder media consists of KO DMEM (Gibco cat. no. A1286101), 10% tet-fbs (Corning cat. no. 35075CV), 1% glutamine (Gibco cat. no. 25030081), and 1% pen/strep (Gibco cat. no. 15140122). After, cells are centrifuged, and the pellet is resuspended in 80/20 media. The cells are then plated onto a T-25 flask that had been coated with 0.1% gelatin (Millipore Cat. no. ES-006-B) for >25min at room temperature and aspirated right before plating. 80 media

consists of 50% Advanced DMEM/F12 (Gibco cat. no. 12634028), 50% Neurobasal-A (Gibco cat. no. 10888022), 1% B27 serum free (Gibco cat. no. 17504044), 1% N2 (Gibco cat. no. 17502048), 1% glutamine (Gibco cat. no. 25030081) and 1% pen/strep (Gibco cat. no. 15140122). 20 media consists of KO DMEM (Gibco cat. no. A1286101), 14% Tet (-) FBS (Corning cat. no. 35075CV), 1% NEAA (Gibco cat. no. 11140050), 1% EmbryoMax Nucleosides (Millipore cat. no. ES-008-D), 1% glutamine (Gibco cat. no. 25030081) and 1% pen/strep (Gibco cat. no. 15140122). 80/20 media consists of 80% 80 media, 20% 20 media, 1000 unit/mL of Mouse LIF (Millipore cat. no. ESG1106), 5mM CHIR99021 (LClaboratory, Fisher cat. no. NO0664823), 10mM PD0325901 (LClaboratory, Fisher cat. no. NO0759248) and 0.1mM of beta Mercaptoethanol (Gibco cat. no. 21985023).

iNIL Cells Differentiated into Motor Neurons

iNIL cells are grown to confluence on a t-25 flask replacing 80/20 media daily. When cells are confluent the flask is washed with HBSS without CAMg (HBSS -/-) (cat. No. 14175095) and trypsinized with 1mL of TrypLE (Gibco cat.no. 12604021). Cells are collected into a 15mL tube with 4mL of feeder media, centrifuged and re-suspended with 1mL AK media without doxycycline to make a single cell suspension. The suspension is diluted with 4mL of AK media without doxycycline and seeded at a cell density of 2.4 million cells on to a 15cm suspension culture dish. This will be EB day 0, two days later the suspension dish is tilted to allow the EBs to sit down towards the bottom of the plate. Approximately 25mL of media is aspirated from the top of the dish careful to not disturb or lose EBs. 25mL of fresh AK media is added to the dish and the total media is measured. Doxycycline is added based on the measured volume, where 1.3uL of 10K x

stock of doxycycline is added to every 12mL of media. All cells are resuspended in the dish before returning to the incubator. Two days later cells are dissociated and plated in motor neuron media, this would represent EB day 4 and MN day 0. To commence dissociation all cells in the suspension dish are collected into a 50mL tube. While the cells pellet in the tube the empty dish is returned to the incubator. Several minutes later, 10mL of clear supernatant from the top of the 50mL tube is used to collect leftover EBs from the empty dish and added to the 50mL tube. The EBs are pelleted at 700rpm for 3min, resuspended in 10mL of HBSS -/- and transferred to a 15mL tube. Cells are pelleted again at 700 rpm for 3min and resuspended gently with 1mL TrypLE using a pipette man. The tube is inverted continuously for 1.5min while cells dissociate. After, 4mL of feeder media is used to deactivate the trypLE and mechanically dissociate the cells. Cells are pelleted at 1000 rpm for 4min and re-suspended with 1mL of AK media to make a single cell suspension. 9mL of AK media is used to pipette mix the cells and are then filtered into a new 15mL tube. Cells are pelleted once again at 1000 rpm for 4min and resuspended in MN media. A cell count at this stage is used to seed cells depending on the assay to be completed. Any dish or plate in which the cells will be seeded on must be coated with Poly-L-Ornithine and incubated overnight prior to use.

AK media consists of Advanced DMEM/F12 (Gibco cat. no. 12634028), Neurobasal-A (Gibco cat. no. 10888022), 13% knockout-SR (Gibco cat. no. 10828028), 55uM bME (Gibco cat. no. 21985023), 1x glutamine (Gibco cat. no. 25030081), and 1x pen/strep (Gibco cat. no. 15140122).

Motor neuron (MN) media consists of Neurobasal-A (Gibco cat. no. 10888022), B27 serum free (Gibco cat. no. 17504044), bME (Gibco cat. no. 21985023), 1x pen/strep (Gibco cat. no. 15140122), 3ug/mL of Doxycycline (Fisher cat. no. AC446060050), 100uM IBMX (Tocris cat. no. 2845), 25uM qVD (MedChemExpress cat. no. HY-12305), 10uM Forskolin (Fisher cat. no. BP2520-5), 4uM Fluorodeoxyuridine (Sigma cat. no. F0503), 4uM uridine (Sigma cat. no. U3003), 10ng/mL GDNF (PeproTech cat. no. 450-10), 10ng/mL BDNF (PeproTech cat. no. 450-02), 10ng/mL CNTF (PeproTech cat. no. 450-13), and 1x glutamine (Gibco cat. no. 25030081). If inducing ferroptosis bME is removed from the media and B2 without AO (Gibco cat. no. 10889038) is used in place of B27 serum free (Gibco cat. no. 17504044).

HT-1080/HT-1080 gALOX5

Cells are cultured in DMEM, 10% FBS, 1% NEAA, 1% Pen/Strep

HEK-293T

Cells are cultured in DMEM, 10% FBS, and 1% Pen/Strep.

All cells were incubated in a tissue culture incubator at 37 °C in a humidified incubator containing 5% CO2.

Chemicals and Antibodies

Erastin (cat. no. E7781), ferrostatin-1 (Fer-1; cat. no. SML0583), propargylglycine (cat. no. P7888), liproxstatin-1 (cat. no. SML1414), and EGTA (cat. no. CAS 99590-86-0) were purchased from Sigma- Aldrich. (1S,3R)-RSL3 (cat. no. HY-100218A) and necrostatin-1 stable (Nec-1s; cat. no. HY-14622) were purchased from MedChem Express (Monmouth Junction, NJ, USA), and staurosporine was from LC Laboratories (Woburn, MA, USA) (cat. no. S-9300). Rabbit antibody against poly (ADP-

ribose) polymerase (PARP) was from Cell Signaling Technology (Danvers, MA, USA; cat. no. 9532), Rabbit antibody against Choline Acetyltransferase was from Abcam (Cambridge, MA,USA; cat. no. ab178850) Rabbit antibody against Class 3 Beta Tubulin was from Cell Signaling Technology (Danvers, MA, USA; cat. no. 5568), Mouse antibody against Hb9 (Mnx1) was from Developmental Studies Hybridoma Bank (Iowa, USA; cat no. 81.5C10), Rabbit antibody against actin was from Santa Cruz Biotechnology (Dallas, TX, USA; cat. no. sc-1616-R), Rabbit antibody against Gapdh was from Developmental Studies Hybridoma Bank (Iowa, USA; cat no. D16H11), secondary antibody against rabbit IgG was from LI-COR Biotechnology (Lincoln, NE, USA; cat. no. 925-68071) and secondary antibody against mouse IgG was from LI-COR Biotechnology (Lincoln, NE, USA; cat. no. 925-68071)

Inducing Ferroptosis in NSC-34 Cells

Assay plates (Corning, cat. no. 3712) were prepared by seeding 2000 NSC-34 cells per well in 40uL of growth medium into black, clear bottom 384-well plates. The assay plate was incubated for 2 days before compound treatment. On the day of the experiment, empty 384-well polypropylene plates (Greiner, Monroe, NC, USA; cat. no. 781281) were filled with 50uL of growth medium except for column 5 where 100uL of lethal solution (20uM of erastin and/or RSL3) was transferred. Then, 2-fold serial dilution of the lethal solution across columns 5–20 was carried out by transferring 50uL of compound solution to the next column successively with mixing. We named this plate as '1x lethal plate'. Culture media in the assay plate were removed, and NSC-34 cells were treated with lethals in a 2- fold dilution series by transferring 40uL of solution from

a ‘1x lethal plate’. The assay plate was returned to the culture incubator and maintained for 24hr before starting a resazurin viability assay.

Inducing Ferroptosis in iNIL MNs

Using the standard differentiation protocol iNIL cells are thawed and grown to confluency in a T-25 flask. They are then seeded to a 15cm suspension culture dish (Corning, cat. no. 430597). 24hr before dissociation a 96 well plate is coated with 1/10 dilution of Poly-L-Ornithine (PLO) and incubated overnight. The next day, before seeding cells, shake off PLO from plate and wash with 100uL autoclaved water; rinse twice with water before use. Cells ready for dissociation are collected and seeded 25,000 cells per well in 100uL MN media. Two 96 well plates are prepared one labeled as ‘high dose’ and the second as ‘low dose’. The first two columns of the ‘high dose’ plate are used as the cells only, positive control and is not treated with any drug. The last two columns of the ‘low dose’ plate contain media only, serving as the negative control. Rows B,C,D will be treated with RSL3 and rows E,F,G will be treated with RSL3 plus compound (fer-1, bME, EGTA, Riluzole, Edaravone, Na4PB) the following day. Rows A and H are filled with 100uL of water to prevent evaporation. 24hr later a ‘2x lethal plate’ is made by filling a 96 well plate with 150uL of MN media excluding rows A, H containing water only and column 3 where 300uL of 2x lethal compound (RSL3 and/or RSL3 + compound) will be used for the serial dilution. In this case 200 nM of RSL3 is the concentration used in column 3. After, 100uL of each well is transferred to the 96 well plate seeded the day before containing MNs. 24hr after treating cells with compound, the standard resazurin viability assay is used to evaluate cell viability.

This assay was used for all iNIL cell viability assays in this study, including treatment with the following compounds: bME, fer-1, EGTA, Riluzole, Edaravone, and Na4PB.

Inducing Ferroptosis in HT-1080

Assay plates (Corning, cat. no. 3712) were prepared by seeding 4,000 HT-1080 cells per well in 20uL of growth medium into black, clear bottom 384-well plates. The same day, compound plates were prepared prior to seeding cells by filling empty 384-well polypropylene plates (Greiner, Monroe, NC, USA; cat. no. 781281) with 40uL of growth medium except for column 5 where 80uL of lethal solution (20uM of erastin and/or RSL3) was transferred. Then, 2-fold serial dilution of the lethal solution across columns 5–20 was carried out by transferring 40uL of compound solution to the next column successively with mixing. We named this plate as '2x lethal plate'. HT-1080 cells were treated with lethals in a 2- fold dilution series by transferring 20uL solution from a '2x lethal plate'. The assay plate was returned to the culture incubator and maintained for 24hr before starting a resazurin viability assay.

Resazurin Viability Assay

After 1 day of compound treatment, resazurin (Sigma- Aldrich, cat. no. R7017) was added to the assay plate to a final concentration of 0.01%. The assay plate was incubated further for 1 day to allow reduction of resazurin, which produced red fluorescence. The fluorescence intensity was determined using a Victor 2 plate reader (Perkin Elmer, Melville, NY, USA) with a 544-nm excitation filter and a 590-nm emission filter. Percentage growth inhibition (% GI) was calculated from the following formula using fluorescence intensity values:

%GI =100 * (1-(X-N)/(P-N)

where X is cells treated with compound, N is growth medium only, and P is cells without any compound.

Light Microscopy

Phase contrast images were obtained using a phase contrast inverted microscope (Motic, Viking Way Richmon, BC, Canada) equipped with a 910 objective. At least three independent fields were acquired for each experimental condition. Representative photographs from one field of view are shown.

Analysis of Lipid Reactive Oxygen Species Generation

NSC-34 cells were seeded in six-well plates and treated with test compounds for the indicated time. On the day of experiment, BODIPYTM581/591 C11 (Thermo Fisher Scientific; cat. no. D3861) was added to each well to the final concentration of 1.5uM and the culture plate was incubated for 20min at 37 °C. Cells were harvested and washed once with Hanks' balanced salt solution (HBSS; Thermo Fisher Scientific, cat. no. 14025092) to remove excess BODIPY-C11 dye. After washing, cells were pelleted by spinning, and the cell pellet was resuspended in 500uL of HBSS. The cell suspension was strained through a 40-uM cell strainer (BD, San Jose, CA, USA), followed by flow cytometry analysis using Guava easyCyte Plus (Milli- pore, Billerica, MA, USA). BODIPY-C11 signal, which reflects the lipid peroxide level, was measured using the FL1 channel. Experiments were performed in biological triplicates, and a representative result is shown.

Gene Expression Analysis by RT-qPCR

Cells were harvested and washed once with HBSS before freeze storing at 80 °C. On the day of experiment, RNA was purified from the cell pellet using the QIAshredder and RNAeasy extraction kits (Qiagen, Germantown, MD, USA) according to the manufacturer's instructions. Two milligrams of total RNA per sample was subsequently used in a reverse transcription reaction using the TaqMan RT Kit priming with Random Hexamers (Thermo Fisher Scientific). The following TaqMan assay primers were purchased from Thermo Fisher Scientific: Actb (assay ID Mm02619580_g1), Ngfr (assay ID Mm00446296_m1), Chat (assay ID Mm01221880_m1), Gria1 (assay ID Mm00433753_m1), Gria2 (assay ID Mm00442822_m1), Gria3 (assay ID Mm00497506_m1), Gria4 (assay ID Mm00444754_m1), Grin1 (assay ID Mm00433790_m1), Grin2a (assay ID Mm00433802_m1), Grin2b (assay ID Mm00433820_m1), Grin2d (assay ID Mm00433822_m1), Mnx1 (a.k.a. Hb9) (assay ID Mm01222622_m1), Isl1 (assay ID Mm00517585_m1), Nefm (assay ID Mm00456200_m1), Map3k5 (assay ID Mm00434883_m1), Lamb2 (assay ID Mm00493080_m1), Itga2 (assay ID Mm00434371_m1), Col16a1 (assay ID Mm01180622_m1), Abcc3 (assay ID Mm00551550_m1), Abca1 (assay ID Mm00442646_m1), Cth (assay ID Mm00461247_m1), Cbs (assay ID Mm00460654_m1), Cyp24a1 (assay ID Mm00487244_m1), Rarb (assay ID Mm01319677_m1), and PPIP5K2 (assay ID Hs00274643_m1). Quantitative PCR was performed on triplicate samples in 96-well format on a Bio-Rad CFX96 Real-Time PCR System (Bio-Rad Laboratories, Hercules, CA, USA). The change in expression of a gene

between experimental and control conditions was computed using the **ΔΔCt** method with Actb as an internal reference gene.

Measuring HB9/GFP Expression in iNIL Cells

iNIL cells are grown following the standard differentiation protocol. To compare differentiated cells with undifferentiated cells, two sets of cells are grown in parallel. One is labeled as 'uninduced' and the other as 'induced'. During the doxycycline treatment stage of differentiation, 'induced' cells follow the standard protocol. Meanwhile, 'uninduced' cells are replaced with fresh media according to the standard protocol but without the addition of doxycycline. 2 days later cells were then dissociated, harvested, and washed once with Hanks' balanced salt solution (HBSS; Thermo Fisher Scientific, cat. no. 14025092). After washing, cells were pelleted by spinning, and the cell pellet was resuspended in 500uL of HBSS. The cell suspension was strained through a 40-uM cell strainer (BD, San Jose, CA, USA), followed by flow cytometry analysis using Guava easyCyte Plus (Milli- pore, Billerica, MA, USA).

Immunostaining iNIL Cells

iNIL cells are incubated overnight in a 96-well plate at 4 degrees Celsius with 1mL of 100% cold methanol. The next day, the media was aspirated and replaced with 1mL HBSS +/+ and incubated for 1hr at 4 degree Celsius. After, 500uL of primary antibody diluted in odyssey blocking buffer was carefully added to each well. Media is added to the surrounding wells to prevent evaporation. The cells are incubated with primary antibody at room temperature for 1hr. Then cells are washed with 1mL of HBSS +/+ twice before adding 480uL of secondary antibody diluted in odyssey blocking buffer. Aluminum foil is used to protect the cells and the antibody from the light. Cells are

incubated at room temperature for 30min. Prepare DAPI (Stem Cell Technologies, cat no.75004) working solution from stock by diluting 300uM DAPI 1:1000 in HBSS +/+ to make 300nm working concentration. Add 500uL of diluted DAPI rocking back and forth to mix. The results can be observed under a fluorescent microscope.

siRNA Transfection

HT-1080 cells were seeded at a cell density of 175,000 cells per well on a 6-well plate. The next day 9uL of Lipofectamine RNA iMAX Reagent was diluted in 150uL of Opti-MEM. In a separate eppendorf tube, 30 pmol of siRNA is diluted in 150uL of Opti-MEM. The diluted siRNA is transferred to the diluted Lipofectamine reagent at a 1:1 ratio and pipette mixed. The complex was left to form at room temperature for 5min, after which, it was added drop wise to one well on a 6-well plate. 48hr later these cells along with non-transfected cells were trypsinized and seeded into a black clear bottom 384-well plate. These assay plates were prepared by seeding 4000 cells in 20uL of growth medium per well. These cells were compound treated the same day of seeding. Empty 384-well polypropylene plates (Greiner, Monroe, NC, USA; cat. no. 781281) were filled with 40uL of growth medium except for column 5 where 80uL of lethal solution (20uM of erastin and/or RSL3) was transferred. Then, 2-fold serial dilution of the lethal solution across columns 5–20 was carried out by transferring 40uL of compound solution to the next column successively with mixing. We named this plate as ‘2x lethal plate’. The HT-1080 cells were treated with lethals in a 2-fold dilution series by transferring 20uL of solution from the ‘2x lethal plate’. The assay plate was returned to the culture incubator and maintained for 24hr before starting a resazurin viability assay.

CRISPR Molecular Cloning

To clone the sgRNA guide sequence into the pLCV2 vector backbone, cut plasmid and dephosphorylate with FastDigest BsmBI and FastAP at 37 °C for 30min with the following:

5ug	lentiCRISPRv2
3uL	FastDigest BsmBI
3uL	Fast AP
6uL	10X Fast digest buffer
0.6uL	100mM DTT (freshly prepared)
XuL	ddH2O
60uL	total

Run the vector on a 0.8% agarose gel for approximately 1hr; excise and gel purify the band. Phosphorylate and anneal the Oligonucleotides by combining the following in an eppendorf tube:

1uL	Oligo 1 (100uM)
1uL	Oligo 2 (100uM)
1uL	10X T4 Ligation Buffer
6.5uL	ddH2O
0.5uL	T4 PNK
10uL	Total

Then anneal by heating to 95 °C for 5min in water bath. Turn off the water bath and let the tubes gradually cool down and leave to anneal overnight. Dilute annealed

oligonucleotides 1:200 the next day. Set up ligation reaction and incubate at room temperature for 10min:

XuL BsmBI digested plasmid (50ng)

1uL Diluted oligo duplex

5uL 2x Quick ligase buffer

XuL ddH2O

10uL subtotal

- Add 1uL Quick ligase for final total of 11uL.

Transfer 2uL of ligation reaction mixture to STBL3 bacteria for transformation, pick colonies, make glycerol stocks and mini prep samples.

Designing Oligos

Benchling was the online tool used to design all oligonucleotides for CRISPR knockouts. For efficient CRISPR knockout it is suggested to design more than one oligonucleotide targeting the same gene but different exons of that gene.

PolyJet Transfection/Lentivirus Production

In a 10cm dish HEK 293T cells were seeded at a cell density of 3.35 x10^6. 24hr later the media was replaced in the dish with 9mL of fresh media. In 500uL of DMEM with high glucose the following was added and pipette mixed: 10ug of transfer plasmid (pLCV2, addgene cat. no. 52961), 7.5ug of packaging plasmid (psPAX2, addgene cat. no. 12260), and 5ug of envelope plasmid (pMD2.G, addgene cat. no. 12259). In a separate tube, 40uL of PolyJet reagent (SignaGen Laboratories cat. no. SL100688) was diluted in 500uL DMEM with high glucose and pipette mixed. The diluted PolyJet reagent was immediately added to the diluted DNA solution all at once, careful not to reverse the

mixing order. The solution was vortex mixed immediately and incubated at room temperature for 10min (*Never keep the complex forming for more than 20min) The complex was added drop wise to the 10cm dish and swirled to mix. 24hr after transfection, the media was aspirated and replaced with fresh media. 48hr after transfection, 9mL of media was harvested in a 50mL tube and 9mL of fresh media was added to the dish. 72hr after transfection, the media was collected again from the dish and added to the 50mL tube collected the day before for a total of 18mL. This viral supernatant was centrifuged at 3,000 rpm for 10min at room temperature. The pellet was discarded, and the viral supernatant was filtered with a 0.45uM low protein binding membrane. The viral supernatant was either used immediately or stored at -20 degrees Celsius.

For iNIL cells, after filtering the viral supernatant, the following additional steps were taken to ultracentrifuge and concentrate the virus: approximately 8mL of the filtered supernatant was aliquoted to 2 ultracentrifuge tubes (ref331372 12.5mL open top). Using the balance to make sure the weight is equal, the supernatants were ultracentrifuged at 16500 rpm for 90min at 4 degrees Celsius in a swinging bucket (SW 41 Ti). The supernatant was decanted into a container with 10 percent bleach. The tubes were covered in parafilm and stored at 4 degrees Celsius overnight. The next day pellets were re-suspended with 500uL of DMEM for a total of 1mL.

CRISPR Knockout HT-1080

HT-1080 cells are seeded at a cell density of 150,000 cells per well in 700uL. The cells are pipette mixed with 1.3mL of viral supernatant and the 2mL are plated onto a 6-

well plate and incubated for 2 days. 48hr later cells are trypsinized and seeded again at 150,000 cells per well in 700uL for a second round of transduction.

For ACSL4 knockout, three 15mL tubes were prepared with 1.3mL of viral supernatant. Two tubes contained viral supernatant targeting ACSL4 exon 3 and one tube with viral supernatant targeting ACSL4 exon 5. The viral supernatant was mixed with 150,000 HT-1080 cells, plated, and incubated for 48hr. On the second round of transduction, three 15mL tubes were prepared with 1.3mL of viral supernatant again. This times two 15mL tubes contained viral supernatant targeting ACSL4 exon 5 and one tube targeting ACSL4 exon 3. The viral sup was mixed with the HT-1080 cells previously transduced such that the following knockouts were generated: HT1080 ACSL4 knockout Exon 3, HT1080 ACSL4 knockout Exon 5, HT1080 ACSL4 knockout Exon 3 and Exon 5. After another 48hr, cells were either puromycin or blasticidin selected depending on vector construct.

CRISPR Knockout iNIL

A 6-well plate is coated with 2mL of 0.1% gelatin for >25min at room temperature and aspirated before use. Confluent iNIL cells are trypsinized from a T-25 flask and 150,000 cells in 1.7mL of media are mixed with 306uL of concentrated viral supernatant and plated on the coated well of the 6-well pate and returned to the incubator. 2 days later cells are trypsinized and transduced again with 306uL of viral supernatant and incubated for another 48hr.

Blasticidin Selection

After transducing cells, they are seeded onto a 6-well plate at a cell density of 75,000 cells per well in media containing 10ug/mL of blasticidin. The controls used for blasticidin selection include untransduced cells as well as cells transduced with empty

plasmid. 48hr after treatment, cells that were not transduced were completely dead and all other cells were growing. These cells are continuously cultured in their corresponding growth media supplemented with 10ug/mL of blasticidin.

CHAPTER 3: RESULTS

NSC-34 Cells Are Sensitized to Ferroptosis Upon Differentiation

NSC-34 is a hybrid cell line: an amalgamation of neuroblastoma and primary spinal cord cells. This combination allows for the differentiation of the cells into a motor neuron-like state; consequently, enabling the characterization of ferroptosis in two distinct cellular conditions. Since ferroptosis sensitivity had not been tested in NSC-34, cells were treated with erastin and RSL3 individually.

Treatment with erastin showed moderate inhibition of growth in NSC-34 cells when utilized at a micromolar range of concentration (Fig. 1A). However, there was no clear cell death suggesting the cell line was somehow resistant to ferroptosis induction via system Xc inhibition. The same drug successfully induced cell death in the control cell line HT-1080, confirming both the potency and integrity of the drug used in this study (Fig. 1B). RT-qPCR confirmed the expression of xCT in the cell line, negating any theories that lack of expression of the gene was the cause of such resistance (Fig. 1D). At this point, erastin alone was not sufficient enough to induce ferroptosis.

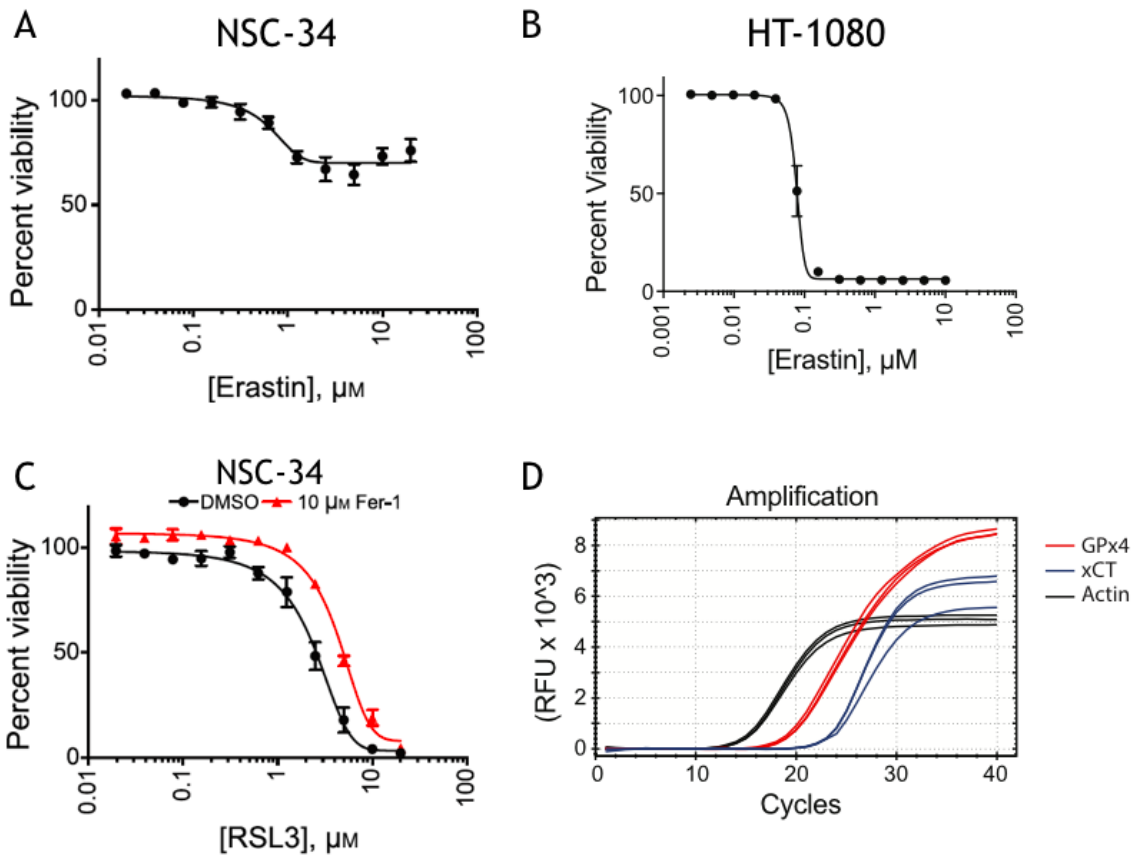

Figure 1: Ferroptosis induction in NSC-34 cell line with erastin and RSL3

Figure 1

Erastin or RSL3 alone do not successfully induce ferroptosis in NSC-34 despite both xCT and GPX4 expression. (A) NSC-34 cells treated with erastin alone did not induce cell death. (B) HT-1080 cells treated with erastin successfully induced ferroptosis confirming erastin was viable. (C) NSC-34 cells were sensitized to RSL3 treatment, but this cell death could not be rescued by fer-1. (D) RT-qPCR showed that NSC-34 cells did express both xCT and GPX4.

Conversely, RSL3 successfully elicited cell death at micro molar range concentration in NSC-34 but this cell death could not be suppressed by ferrostatin-1(fer-

1), a known inhibitor of ferroptosis (Fig. 1C). In the control cell line, HT-1080, cell death was induced by RSL3 and rescued by fer-1 (Fig. 2A). RT-qPCR validated expression of gpx4 in NSC-34 suggesting that the mechanism of action of RSL3 was not compromised (Fig. 1D). The reason for lack of inhibition of fer-1 could be attributed to a deficiency in molecular components essential to carrying out the ferroptotic pathway, such as the presence of iron. Iron plays a significant role in carrying out ferroptosis as it generates lipid peroxides via Fenton chemistry or as a cofactor for lipid oxidizing enzymes. Therefore, cells were treated with a combination of erastin and RSL3 in the presence of ferric citrate which would provide extracellular iron to facilitate effective carryout of the pathway (Fig. 2B). Not only were cells susceptible to the treatment, but they were also rescued by fer-1, indicating that ferroptosis was the major pathway at play (Fig. 2C).

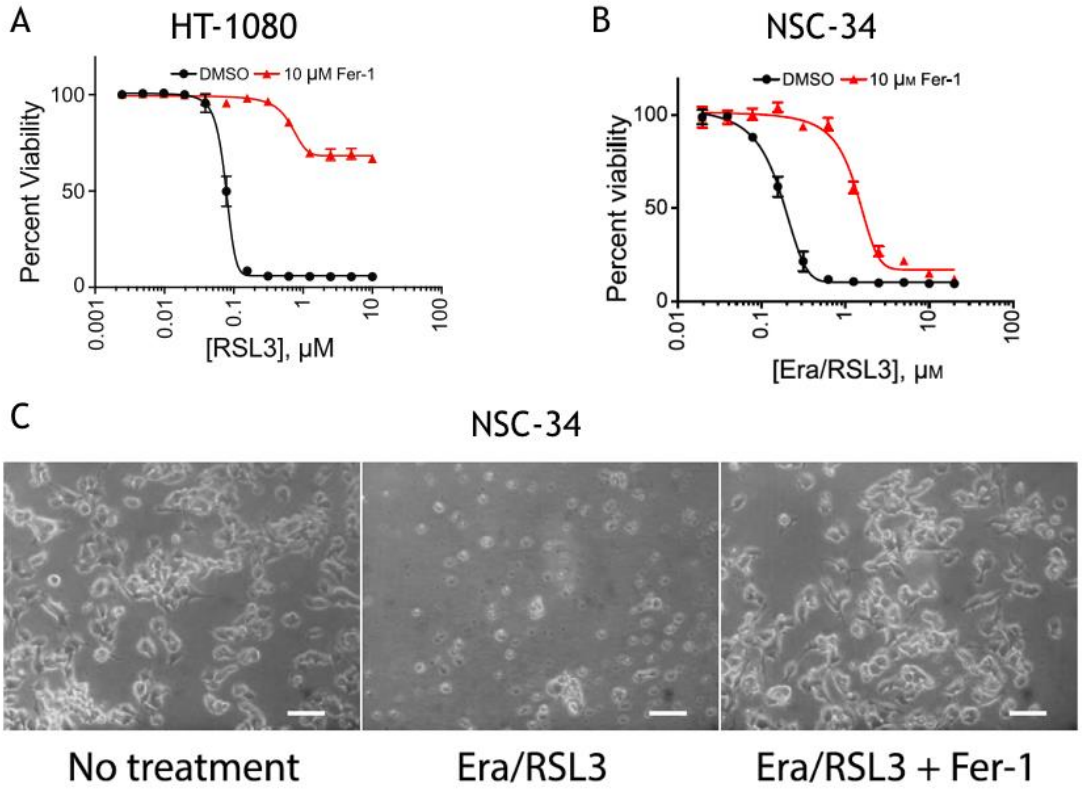

Figure 2: Optimal condition to induce ferroptosis in NSC-34

Figure 2

Erastin, RSL3 and 50 µg·mL^{-1} ferric citrate was the optimal cocktail to induce ferroptosis in NSC-34. (A) HT-1080 cells are sensitized to RSL3 and the cell death is inhibited by fer-1 showing the integrity of the compounds used in this study. (B) The cocktail Erastin, RSL3 and 50 µg·mL^{-1} ferric citrate was the best method to induce ferroptosis in NSC-34 cells and this cell death could be inhibited with fer-1. (C) Cell death with FINs is visually represented as well as inhibition of cell death by fer-1.

To further establish that ferroptosis was the major cell death modality involved, lipid ROS was measured using a BODIPY assay. This assay showed a significant increase of lipid ROS in cells that were treated with the cocktail when compared to the DMSO control (Fig. 3A). A Parp assay confirmed that the cell death induced by the cocktail was non-apoptotic since the Parp protein was not cleaved after immunoblotting (Fig 3B). In comparison, NSC-34 cells treated with staurosporine (STS), an apoptosis inducer, did show Parp cleavage (Fig 3B). Moreover, cells treated with caspase inhibitors or necroptosis inhibitors such as zVAD-fmk or Necrostatin-1 (Nec-1) respectively, did not suppress the cell death (Fig. 3C). However, the ferroptosis inhibitor Liproxstatin-1 did inhibit cell death induced by ferroptosis similar to fer-1 (Fig. 3C) This data indicates that other cell death modalities such as apoptosis and necroptosis are not induced by the cocktail. Hence, the optimal condition to test ferroptosis sensitivity in the NSC-34 cell line is with a combination of erastin, RSL3 and ferric citrate.

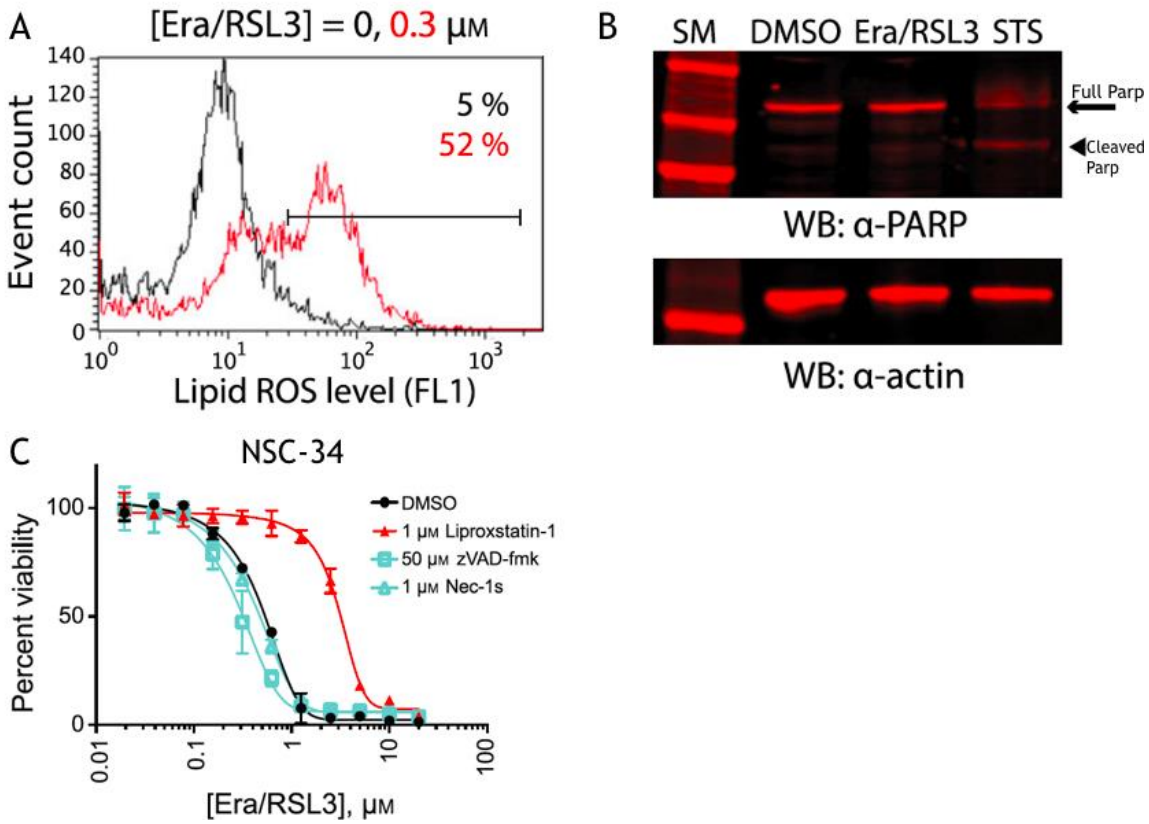

Figure 3: Cell death induced by FINs is ferroptosis specific

Figure 3

Ferroptosis is the main form of cell death induced by the cocktail Erastin, RSL3 and 50 μg·mL^{-1} ferric citrate. (A) Increase in Lipid ROS in cells treated with FINs show that ferroptosis is the main cell death modality involved. (B) Lack of PARP cleavage in cells treated with FINs suggest cells are dying via a non-apoptotic route. Cells treated with staurosporine (STS) were used as the control as there was successful PARP cleavage. (C) Cells treated with FINs and either necroptosis or apoptosis inhibitors did not show suppression of cell death. However, cells treated with the ferroptosis inhibitor Liproxstatin-1 showed suppression of cell death induced by FINs.

Now that an effective way to measure ferroptosis sensitivity in the NSC-34 cell line was determined, analyzing if there were differences in sensitivity upon differentiating the cells into a motor neuron-like state was crucial to understanding the pathway in multiple contexts. In order to begin this investigation, establishing the optimal differentiation condition was imperative. The literature has suggested several conditions in which to differentiate the cell line; leading to the morphological and genetic analysis of the cells in several conditions.

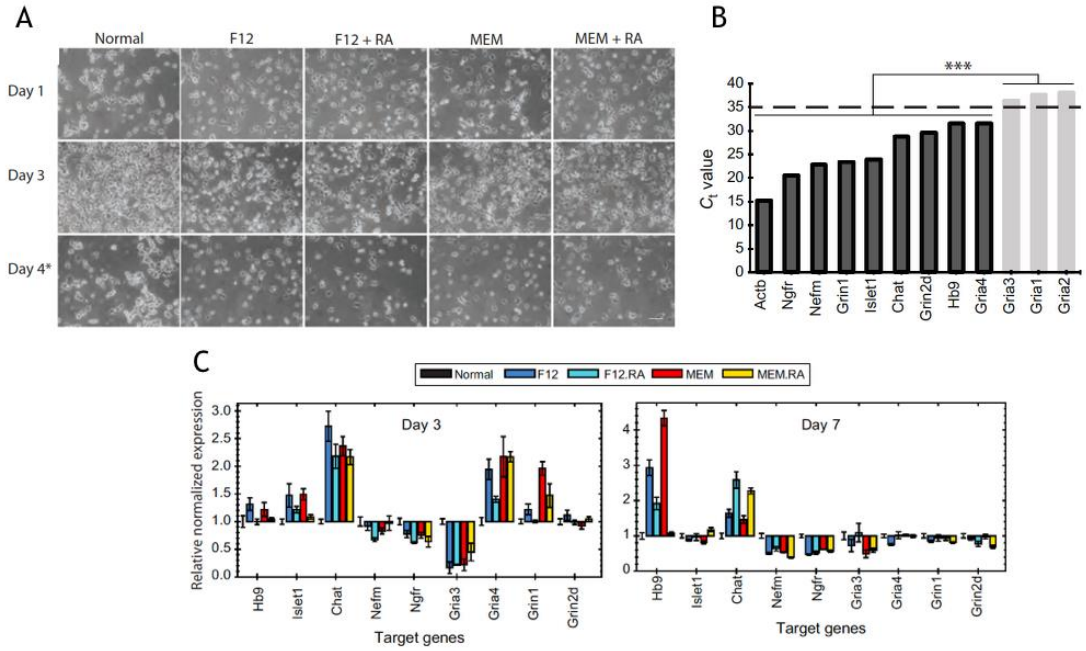

Figure 4: Optimal condition to differentiate NSC-34 into a motor neuron-like state

Figure 4

MEM 1% FBS without all trans retinoid acid incubated for three days was the optimal differentiation condition. (A) All differentiation conditions present the same motor neuron-like morphology. (B) Genes with low expression were excluded from determining the optimal differentiation condition. (C) RT-qPCR shows the upregulation and

downregulation of neuronal markers based on differences in basal media as well as time frame of differentiation.

Morphologically, differentiation in NSC-34 manifests itself by forming neurites, elongated projections stemming from the cell body. This particular feature was consistent for all differentiation conditions (Fig. 4A). Genetically, there were variations in differentiation depending on basal media as well as time frame of differentiation. Therefore, cells were differentiated under multiple conditions in order to select the optimal condition. Normal cells or undifferentiated cells were cultured in DMEM 10% Fetal Bovine Serum (FBS). Differentiated cells were cultured under four separate conditions: DMEM/F12 1% FBS, DMEM/F12 1% FBS with all-trans retinoid acid, MEM 1% FBS, and MEM 1% FBS with all-trans retinoid acid. Cells were differentiated under each condition for three days and seven days. At each time point, cells were harvested and using RT-qPCR probed for upregulation of neuronal markers. Prior to selecting the optimal differentiation condition, genes with low expression levels were excluded from the analysis (Fig. 4B). It was deduced that longer differentiation times such as seven days led to a downregulation of neuronal markers, whereas a shorter differentiation time frame of three days led to an upregulation of neuronal markers: Islet1, Chat, Gria4, and Grin1. Furthermore, the basal media consisting of MEM 1% FBS without all trans retinoid acid presented as the condition with the most consistent upregulation of neuronal markers (Fig. 4C). As a result, cells differentiating for three days in MEM 1% FBS without all trans retinoid acid were selected as the optimal differentiation condition.

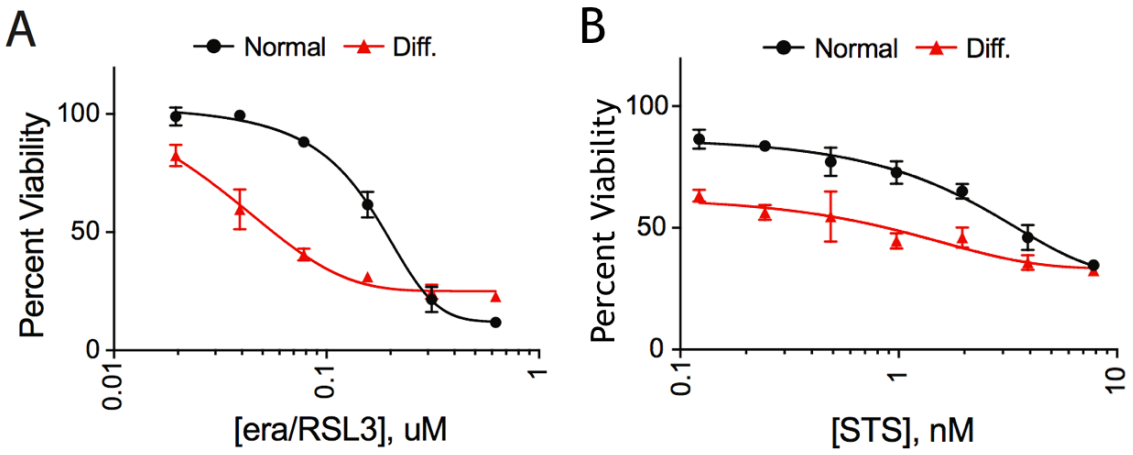

Figure 5: NSC-34 differentiated cells are more sensitive to cell death

Figure 5

Differentiated cells are sensitized to cell death inducers. (A) Differentiated cells are more sensitive to FINs than normal cells. (B) Differentiated cells are also more sensitive to the apoptosis inducer staurosporine (STS) than normal cells.

Undifferentiated cells were compared to differentiated cells in terms of ferroptosis sensitivity by employing a cell viability assay. All cells were treated with a two-fold dilution of a cocktail of ferroptosis inducers (FINs) to generate a dose response curve. Normal cells were less sensitive to ferroptosis when compared to its differentiated counterpart (Fig. 5A). These results elicited the question whether or not this amplified sensitivity in differentiated cells was specific to ferroptosis. For this reason, both normal and differentiated cells were treated with the apoptosis inducer staurosporine. Upon apoptosis induction, differentiated cells were also more sensitive to cell death than the normal cells (Fig. 5B). Therefore, the cell death sensitivity in NSC-34 differentiated cells

was not specific to ferroptosis but warranted an investigation as to why these cells were more susceptible to cell death than normal cells.

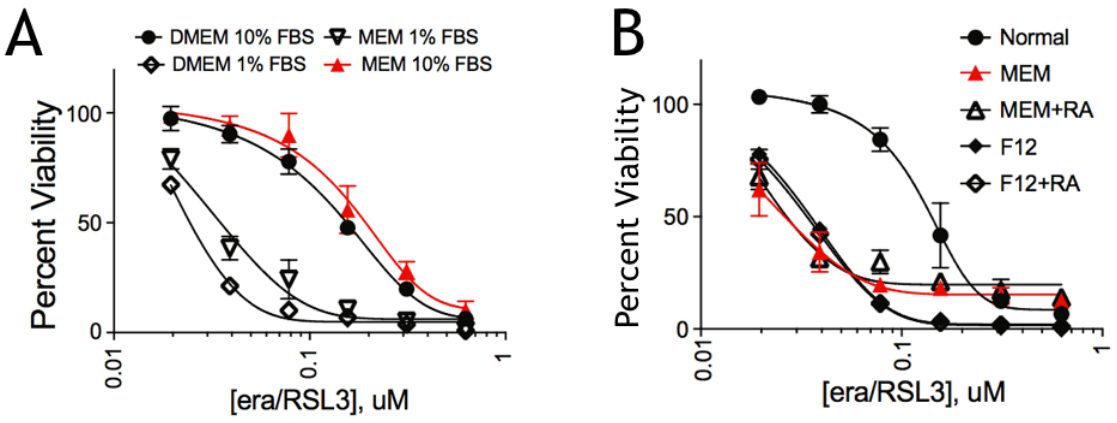

Figure 6: Extrinsic factors involved in NSC-34 sensitivity differences

Figure 6

Antioxidant properties in FBS influences NSC-34 ferroptosis susceptibility. (A) Basal media does not affect sensitivity in differentiated cells but rather the amount of FBS influences this sensitization. (B)Neither basal media nor the presence or absence of all trans retinoid acid affects sensitization in differentiated cells.

Comparing the two cellular conditions there were definitive external differences that were immediately apparent, such as the media conditions. Thus, each component of the media was tested as a potential extrinsic factor causing the sensitivity changes. The basal media and presence or absence of all trans retinoid acid had no effect on sensitization of the cells (Fig. 6B). However, the quantity of fetal bovine serum did affect sensitization (Fig 6A). Cells cultured in 10% FBS were more resistant to cell death, whereas cells cultured in 1% serum had a significant change in susceptibility to ferroptosis (Fig 6A).

These results are attributed to antioxidant properties in the serum protecting the cells from death in conditions that were ten-fold higher than the differentiated cells.

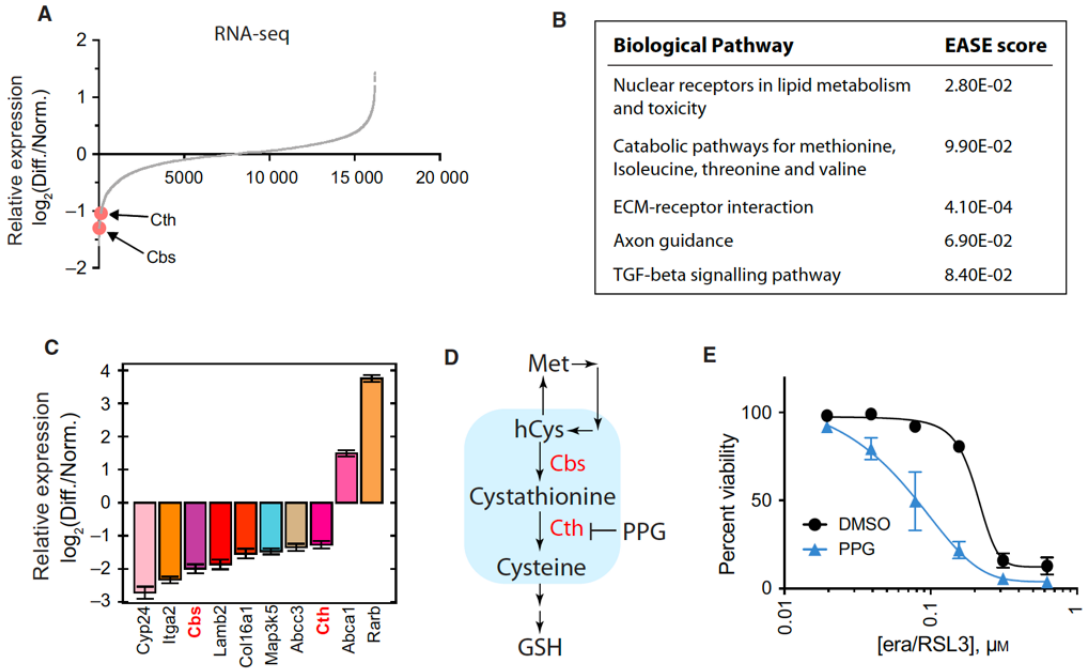

Figure 7: Intrinsic factors involved in NSC-34 sensitivity differences

Figure 7

David analysis reveals Cth and Cbs downregulation is an intrinsic factor sensitizing differentiated NSC-34 cells to ferroptosis. (A) RNA-seq returns the genes upregulated and downregulated by two-fold in differentiated NSC-34 cells versus undifferentiated cells. (B) David software returns the pathways involved in these gene expression changes with emphasis on the catabolic pathways for methionine, isoleucine, threonine and valine. (C) The downregulation of the genes Cth and Cbs are confirmed with RT-qPCR. (D) PPG is a TS pathway inhibitor as an inhibitor of Cth and consequently inhibiting the conversion of cystathionine to cysteine. (E) Normal cells treated with FINs are compared

to normal cells treated with both FINs and PPG showing increase sensitization to ferroptosis in cells where the TS pathway is inhibited.

Although extrinsic factors seemed to play a major role in sensitivity changes, it is possible that certain intrinsic pathways could contribute to the results. Therefore, RNA-seq revealed gene expression changes in differentiated cells; these gene expression changes were confirmed with RT-qPCR (Fig. 7A, Fig. 7C). The genes that were upregulated or downregulated two-fold were analyzed using DAVID software. DAVID revealed several biological pathways that are manipulated as a result of the fold changes. These pathways include nuclear receptors in lipid metabolism, catabolic pathways for methionine, isoleucine, threonine, and valine, ECM- receptor interaction, axon guidance, and TGF-beta signaling pathway. Out of the five pathways, the catabolic pathways for methionine, isoleucine, threonine, and valine were of most interest because of its involvement in the Transsulfuration Pathway (TS Pathway) (Fig. 7B). In the TS pathway, intracellular methionine is converted into cysteine, an important component of GSH and indirect influencer of GPX4 function as previously mentioned (Fig. 7D). Differentiated NSC-34 cells have a downregulation of this pathway as a result of the downregulation of the genes Cystathionine Gamma-Lyase (CTH) and Cystathionine Beta-Synthase (CBS). The downregulation of such genes indirectly affects GPX4 function and also affects GSH production leading to an increase in susceptibility to lipid ROS and ferroptosis. Ergo, the downregulation of the TS pathway is an intrinsic factor sensitizing the differentiated cells to ferroptosis. To solidify this connection, undifferentiated cells were treated with FINs and co-treated with PPG or DMSO as the control. PPG is a Cth inhibitor and by

comparison a TS pathway inhibitor. Normal cells treated with PPG and FINs experienced more sensitivity to ferroptosis when compared to the control (Fig. 7E). This sensitivity mirrored the differentiated cells susceptibility to FINs without PPG co-treatment verifying the significance of the downregulation of Cth and Cbs in differentiated cells.

In the NSC-34 cellular model, it was deduced that there were in fact sensitivity changes after differentiating the cells due to both extrinsic and intrinsic factors. Antioxidant properties in FBS confers resistance to ferroptosis in non-differentiated cells and genes in the transsulfuration pathway are downregulated upon differentiation. This piqued interest into the role of ferroptosis in other cellular models such as mouse embryonic stem cells that could be successfully differentiated into motor neurons.

Embryonic Stem Cells Differentiated into MNs Are Sensitized to Ferroptosis

iNIL cells are a doxycycline inducible mouse embryonic stem cell line containing a polycistronic expression construct with the three transcription factors: Neurogenin 2 (Ngn2), Insulin gene enhancer protein (Isl1), and LIM Homeobox 3 (Lhx3).[9] These transcription factors are activated upon doxycycline induction and are sufficient enough to effectively program cells into spinal motor neurons.[9]

During this differentiation process, the iNIL cells are grown to confluency and seeded to a suspension culture dish in AK media where cells can begin to form embryoid bodies (EBs), three dimensional aggregates (Fig. 8A). This stage of differentiation can be referred to as EB day 0 (Fig. 8A). Two days later these embryoid bodies are treated with doxycycline to promote the differentiation of cells into MNs; this stage being referred to as EB day 2 (Fig. 8A). Furthermore, 48hr post doxycycline treatment, cells are dissociated and plated in MN media. During this stage, cells are at MN day 0 or EB day

4, requiring another two days for a morphological representation of MNs (Fig. 8A). Morphologically, one can observe the differences of each stage (Fig. 8B). Interestingly, the differentiation of iNIL cells is confirmed both morphologically and through genetic analysis.

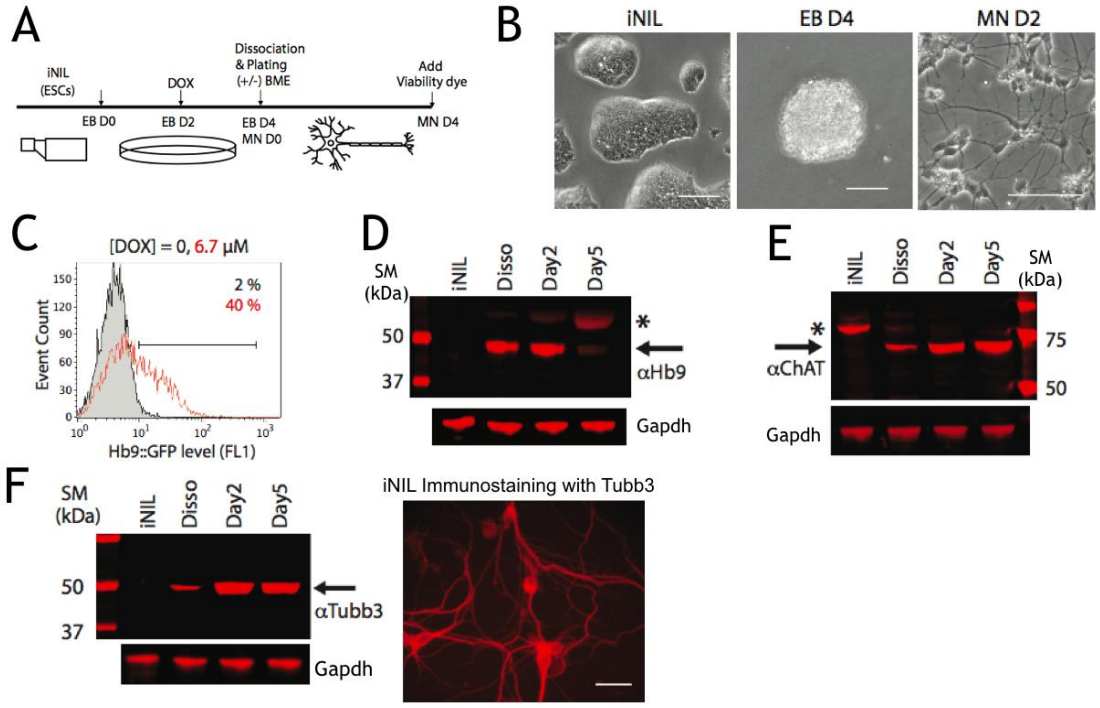

Figure 8: iNIL mouse embryonic stem cells are differentiated into MNs

Figure 8

iNIL cells are efficiently differentiated into MNs. (A) iNIL cells are aggregated into EBs and differentiated into MNs. (B) The morphological differences between iNIL cells, EBs and MNs can be observed. (C) FACs analysis shows an increase in Hb9 as a result of a direct increase in gfp expression in early MN cultures. (D) Significant expression of Hb9 is observed in early MN cultures but decreases as the MNs mature. Asterisk denotes a nonspecific band. (E) The mature MN marker Chat shows increased expression in MNs

over time. Asterisk denotes a nonspecific band. (F) Mature MN marker Tubb3 shows increased expression in MN Day 2 and MN day 5. Immunostaining with Tubb3 antibody reveals a visual manifestation of the Tubb3 gene as the formation of MN axons and dendrites

---

Genetically, neuronal markers can be probed for expression changes in the different stages of development into motor neurons. iNIL cells contain a green fluorescence protein (gfp) transgene driven by the Hb9 promoter where an increased expression of Hb9 directly correlates with an increased expression of gfp, a fluorescence that can be measured using flow cytometry. After the addition of 6.7uM of doxycycline there was a 40% increase in gfp expression measured by FACS analysis which directly correlated with the increase of Hb9 (Fig. 8C). Hb9 is an early motor neuron marker that promotes the differentiation of cells into motor neurons and represses the adjacent population of V2 interneurons[10]. This increase in Hb9 expression is an early event imperative in successful differentiation of the stem cells into motor neurons. Immunoblotting confirmed no expression of the Hb9 protein in iNIL cells but increased expression in dissociated cells which would correspond to MN culture day 0 as well as two days after dissociation or MN Day 2 (Fig. 8D). However, five days after dissociation there is a decrease in expression of Hb9 which is to be expected because as essential as this increase is for differentiation to initiate the change, it is solely an early event (Fig. 8D).

Therefore, other neuronal markers must be probed for expression changes to ensure successful differentiation. Choline acetyltransferase (ChAT) is an enzyme involved in the synthesis of the neurotransmitter acetylcholine and serves as a neuronal

marker for mature motor neurons[11]. Immunoblotting results show that iNIL cells do not express the ChAT protein but cells after dissociation have moderate expression (Fig. 8E). MN day 2 and MN day 5 show a significant increase in ChAT expression showing the progression of the cells into mature motor neurons over time (Fig. 8E). Similar results were obtained for Class III Beta-Tubulin (Tubb3), an important protein involved in the formation of microtubules, more specifically in the formation and growth of axons and dendrites.[12,13] An immunoblot revealed that iNIL cells do not express the protein Tubb3, while dissociated cells have some expression of the protein; MN day 2 and MN day 5 have a significant increase in expression of the Tubb3 protein (Fig. 8F). All immunoblots used Gapdh as the housekeeping protein, serving as the loading control. Morphologically, the development of the embryonic stem cells into motor neurons by forming axons and dendrites is prominently influenced by the expression of Tubb3; a manifestation that is observed through immunostaining with Tubb3 (Fig. 8F). This data suggests the successful differentiation of embryonic stem cells into motor neurons, establishing a viable cellular model to investigate ferroptosis sensitivity in MNs.

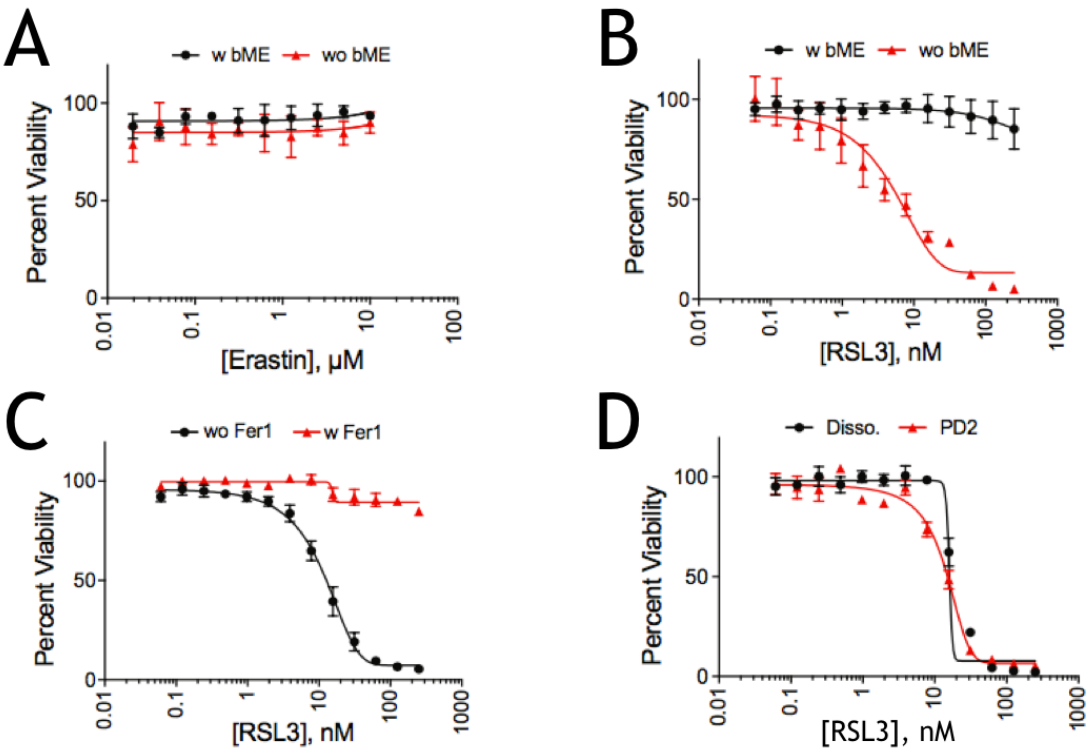

Figure 9: MNs are sensitized to ferroptosis via RSL3 induction

Figure 9

MNs are sensitized to ferroptosis induction via RSL3 an event inhibited by fer-1 and bME. (A) MNs are not sensitized to ferroptosis via erastin treatment. (B) MNs are sensitized to ferroptosis induced with RSL3 treatment. This sensitivity is suppressed with the ferroptosis inhibitor bME. (C) Fer-1 also inhibits ferroptosis sensitivity in MNs. (D) EBs post dissociation show no difference in sensitivity to RSL3 when compared to MNs at Day 2 of culture

---

iNIL cells were differentiated into motor neurons and tested for ferroptosis sensitivity with erastin and RSL3 individually. Cells subject to erastin treatment at the micro molar range of concentration showed no significant cell death or change in viability irrespective of the presence or absence of beta-Mercaptoethanol (BME) (Fig. 9A). This data coincides with the lack of xCT expression in iNIL cells, the target

exploited by erastin to induce ferroptosis. However, cells treated with RSL3 on the nanomolar range of concentration showed ample sensitivity resulting in cell death and a reduction in viability (Fig. 9B). This cell death was rescued when cells were treated with both RSL3 and BME (Fig. 9B). BME is a known ferroptosis inhibiter as it promotes cellular uptake of cystine, an integral component in GSH and overall antioxidant functionality. Differentiated cells susceptible to RSL3 treatment were also treated with fer-1, an inhibitor that successfully rescued cellular death (Fig. 9C). This data suggests that the cellular death occurring in the differentiated cells is a direct result of the ferroptotic pathway.

Since the NSC-34 motor neuron-like model system showed significant differences in normal and differentiated conditions in regard to ferroptosis sensitivity as well as other cell death modalities, it was imperative to assess this in iNIL differentiated cells. Cells post dissociation with an EB morphology were compared to cells two days post dissociation which harbor a MN morphology. In terms of sensitivity to ferroptosis, there was no significant difference between the two distinct stages of differentiation, suggesting this model is effective in both inducing ferroptosis and studying the pathway in MN context (Fig. 9D).

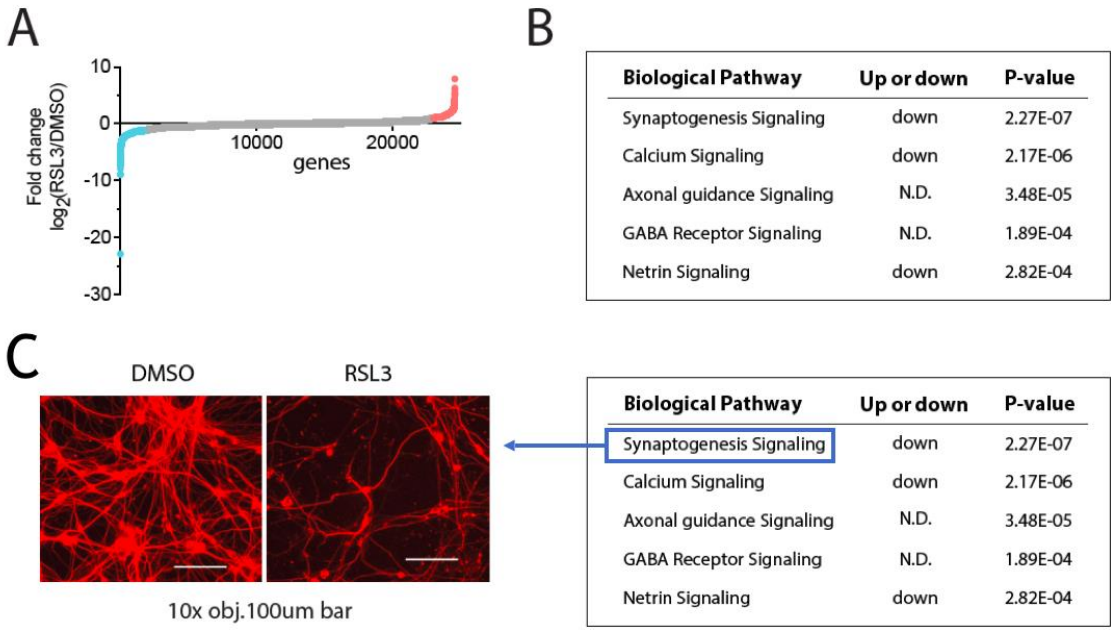

Figure 10: IPA analysis reveals pathways involved in MN sensitivity to ferroptosis

Figure 10

IPA *analysis suggests pathways involved in sensitizing MNs to ferroptosis. (A) RNA-seq returns the genes upregulated and downregulated by two-fold in MNs treated with RSL3 versus MNs treated with the DMSO control. (B) IPA software by QIAGEN returns the pathways involved in these gene expression changes. (C) Morphological reduction of synapses in cells treated with RSL3*

Now that a viable cellular model exemplifies motor neuron sensitivity to ferroptosis, it is essential to find genetic reasons for a lack of resistance to this particular form of cell death. This led to an investigation in fold changes of genes in differentiated cells with and without RSL3 treatment. Similar to NSC-34, RNA-seq data returned the two-fold upregulated and two-fold downregulated genes that were then input into Ingenuity Pathway Analysis (IPA) software for analysis of potential pathways involved (Fig. 10A). These biological pathways included: Synaptogenesis signaling pathway,

Calcium signaling, Axonal guidance signaling, GABA receptor signaling, and Netrin signaling (Fig. 10B). Why these specific pathways were implicated in the sensitivity of MNs to FINs remains to be determined.

Synaptogenesis signaling pathway refers to the genes involved in the formation of synapses between neurons and therefore plays a major role in the nervous system and in the efficient functioning of MNs. Upon ferroptosis induction in MNs via RSL3, there is a significant reduction in the formation of synapses corresponding to significant cellular death which is compatible with the RNA-seq data that shows the genes in this pathway are downregulated (Fig. 10C).

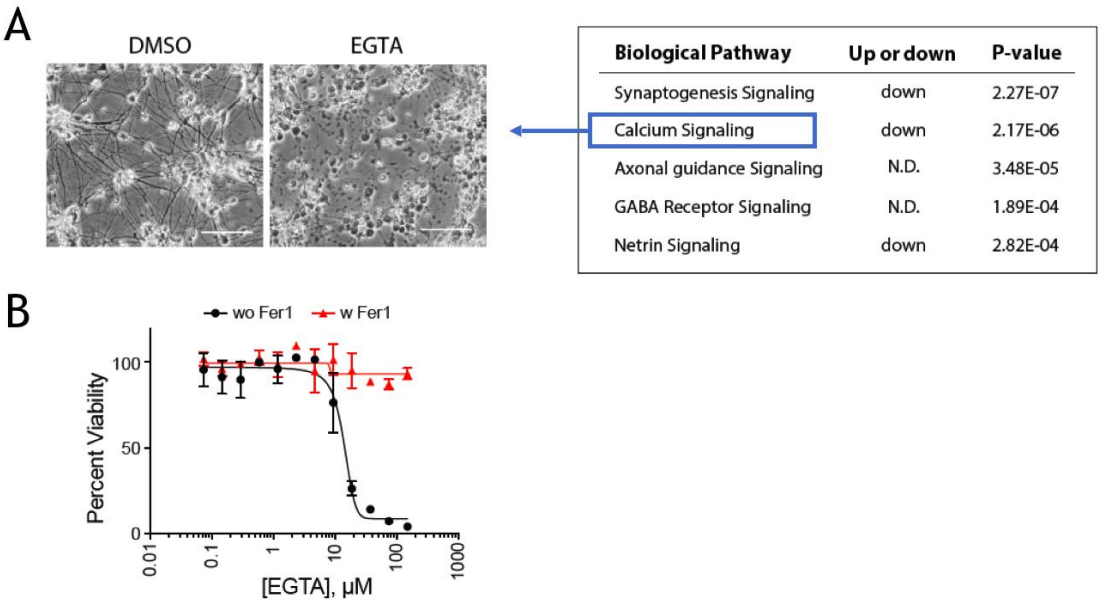

Biological Pathway	Up or down	P-value
Synaptogenesis Signaling	down	2.27E-07
Calcium Signaling	down	2.17E-06
Axonal guidance Signaling	N.D.	3.48E-05
GABA Receptor Signaling	N.D.	1.89E-04
Netrin Signaling	down	2.82E-04

Figure 11: Downregulation of calcium signaling pathway drives ferroptosis in MN context

Figure 11

Calcium signaling downregulation drives ferroptosis. (A) Electron micrographs of iNIL MNs treated with DMSO and EGTA (B)iNIL MNs co-treated with EGTA and fer-1 inhibit cell death

Calcium signaling pathway is another integral component in MNs as calcium (Ca(2+)) participates in the depolarization of the cell. The calcium signaling pathway is implicated in MNs sensitized to ferroptosis, returning as one of the several pathways downregulated in RNA-seq data, but whether its mechanism of action is to protect cells or sensitize cells to ferroptosis is elusive leading to further investigation. Thus, cells were treated with ethylene glycol tetra acetic acid (EGTA), a calcium chelator responsible for depleting intracellular calcium. Morphologically, MNs treated with EGTA appear unhealthy and with no formation of synapses (Fig. 11A). Furthermore, MNs treated with EGTA in the presence of ferroptosis inhibitor fer-1 show a suppression of cell death and a rescue in cell viability suggesting that the mechanism of action of calcium signaling pathway is to drive ferroptosis (Fig. 11B).

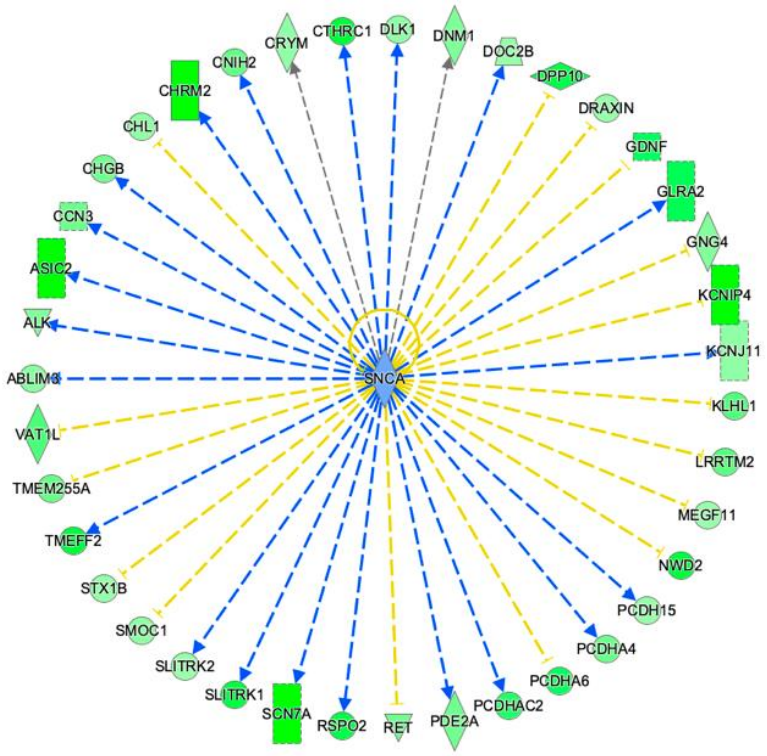

Figure 12: IPA Analysis suggests upstream regulator of downregulated genes

Figure 12

IPA *analysis suggests the upstream regulator of downregulated genes. (A) Snca is returned by the IPA Software as the upstream regulator of downregulated genes*

After specific pathways were determined to be affected by ferroptosis in MNs beginning the groundwork for the pathway's characterization in neuronal context, it is important to understand which specific genes are involved as key regulators. IPA Analysis not only puts into context the genes that are being affected but can also return an upstream regulator, pinpointing the gene responsible for the cascade of deregulation. In this iNIL MN model, Alpha-Synuclein (Snca) was returned as the upstream regulator of downregulated genes (Fig. 12). Since there is no way to easily test the role of Snca in MN sensitivity to ferroptosis, a genetic tool is required to manipulate the gene and understand its function. As a result, the HT-1080 cell line or the parental cell line of ferroptosis was employed in order to evaluate the best genetic tool to verify not only Snca but several genes that could serve as prospective targets for novel therapies in disease contexts where ferroptosis plays a major role, including but not limited to Acyl-CoA Synthetase Long Chain Family Member 4 (ACSL4) and Diphosphoinositol Pentakisphosphate Kinase 2 (PPIP5K2)

PPIP5K2 Knockdown Inhibits Cell Death Induced by Ferroptosis

The genetic testing to further characterize ferroptosis began with small interfering RNA (siRNA), an application useful in implementing knock downs in protein coding genes, with PPIP5K2 as the first target. Diphosphoinositol Pentakisphosphate Kinases (PPIP5Ks) are genes important in forming the enzymes that catalyze the formation of Inositol Pyrophosphates (InsPs), energy rich signaling molecules that regulate a variety of cellular processes including vesicle trafficking and apoptosis.[14] PPIP5Ks exist in

mammals as two isoforms PPIP5K1 and PPIP5K2 and work in conjunction with Inositol Hexakisphosphate Kinases (IP6Ks) of which there are three isoforms in mammals IP6K1, IP6K2 and IP6K3.[14] Together these kinases are essential in forming Inositol Pyrophosphates via the following two pathways: PPIP5Ks phosphorylate Insp6 at position one to produce 1-Insp7; IP6Ks in turn phosphorylate 1-Insp7 at position five to produce Insp8 (Fig. 13A).[14] Alternatively, IP6Ks can phosphorylate Insp6 at position five to form 5-Insp7 which is then phosphorylated at position one by PPIP5Ks to form Insp8 (Fig. 13A).[14] Thus, PPIP5Ks and IP6Ks are kinases that phosphorylate substrates to generate InsPs which are high energy signaling molecules that maintain cellular homeostasis by facilitating essential processes. The pathway that the PPIP5K and IP6K Kinases manipulate requires further investigation and piqued interest on the potential role of PPIP5Ks in the ferroptotic pathway.

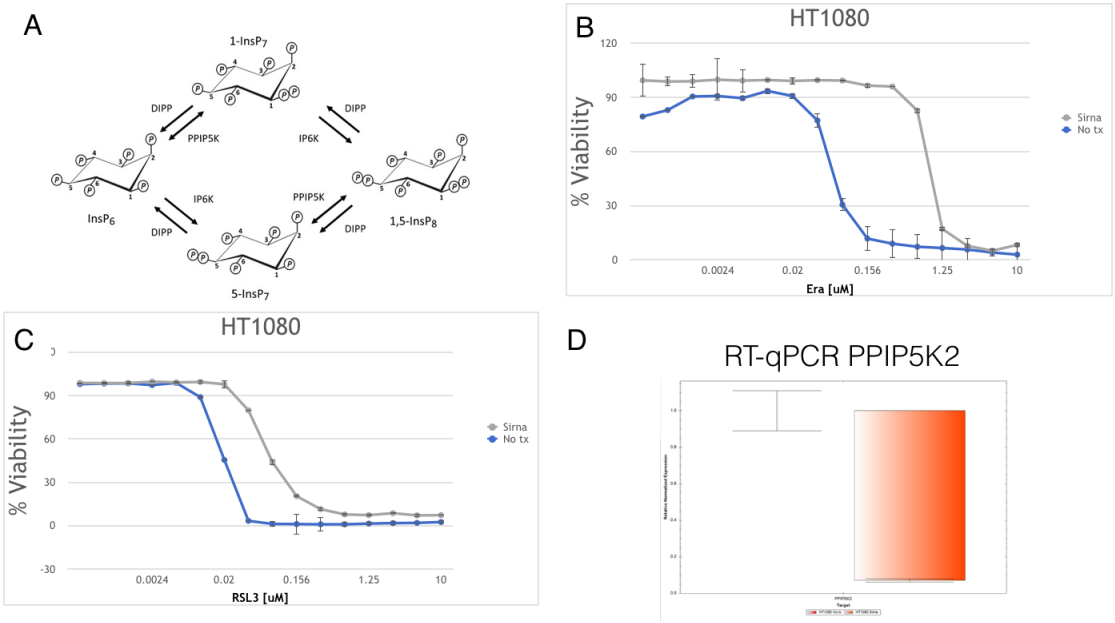

Figure 13: siRNA knockdown of PPIP5K2 inhibits ferroptosis

Figure 13

Silencing PPIP5K2 inhibits ferroptosis. (A) PPIP5Ks route to form the signaling molecules InsPs. (B) HT-1080 cells where PPIP5K2 was silenced via Lipofectamine transfection are compared to cells still expressing PPIP5K2 in terms of sensitivity changes to erastin. HT-1080 cells with siPPIPK2 showed resistance to ferroptosis induction. (C) Same as in (B), except the ferroptosis induction in this case was elicited with RSL3 treatment. Again, HT-1080 cells with siPPIP5K2 show resistance to ferroptosis. (D). RT-qPCR shows downregulation of PPIP5K2 in cells transfected with siRNA for the gene.

PPIP5K2 is a gene that encodes a member of the histidine acid phosphatase family of proteins.[15] Despite containing a histidine acid phosphatase domain, the encoded protein functions as an inositol pyrophosphate kinase, and is thought to lack phosphatase activity. To investigate how this gene might play a role in ferroptosis it was silenced via

siRNA Lipofectamine transfection in the HT1080 cell line. After silencing PPIP5K2, the downregulation of the gene was measured and confirmed with RT-qPCR (Fig. 13D). Ferroptosis sensitivity levels in the HT-1080 cell line were compared in cells expressing PPIP5K2 and in cells where the gene was downregulated. Cells were treated with erastin on the micro molar range of concentration and the cell line that still expressed PPIP5K2 showed ample sensitivity to ferroptosis (Fig. 13B). In contrast, cells where the gene had been downregulated showed significantly less sensitivity, rescuing cell death to an extent similar to that of an inhibitor of ferroptosis (Fig. 13B). Cells treated with RSL3 on the micro molar range of concentration were susceptible to cell death via ferroptosis and the cells where the gene was silenced displayed moderate inhibition of cell death (Fig. 13C). This data suggests that this gene is important in driving the ferroptotic pathway and its absence can suppress this particular cell death modality. However, since siRNA of the PPIP5K2 gene did not generate a complete knockout, in order to fully understand the importance of this gene and other genes involved in ferroptosis, a modern genetic engineering approach known as Clustered Regularly Interspaced Short Palindromic Repeats (CRISPR) was tested and optimized in both HT-1080 and iNIL cells.

CRISPR Knockouts Provide Stable Cell Lines for Genetic Studies in HT-1080

Clustered Regularly Interspaced Short Palindromic Repeats (CRISPR) and CRISPR-associated protein 9 (Cas9) create an efficient genetic engineering approach for permanent gene knockouts or knock-ins. This technology harnesses the immune system of bacteria, more specifically, the Cas9 enzyme was isolated from Streptococcus pyogenes.[16] This enzyme is an endonuclease with non-specific targets, thus requiring a guide RNA (sgRNA) to guide the enzyme to a specific genetic locus. This attribute

allows the manipulation of any gene of interest as long as the integrity and design of the sgRNA itself meets the appropriate standards.

sgRNAs are comprised of two components, a CRISPR RNA (crRNA) and a trans-activating CRISPR RNA (tracrRNA).[16] The crRNA is a 17-20 nucleotide sequence complimentary to the target DNA and the tracrRNA serves as a binding scaffold for the Cas9 endonuclease.[16] The crRNA and tracrRNA exist independently in nature but can be synthetically combined to generate single guide RNAs (sgRNA).[16] sgRNAs are single RNA molecules that contain the custom designed crRNA sequence fused to the scaffold tracrRNA sequence, simplifying the genetic engineering approach.[16] Although there are several CRISPR methods, the CRISPR Cas9 along with sgRNAs were the selected approach for introducing CRISPR knockouts and overexpressing cDNA in both HT-1080 and iNIL cells via lentiviral transduction. Since sgRNAs are responsible for guiding the enzyme to a specific genetic locus, its design is imperative to facilitate a successful CRISPR knockout. The first parameter to consider when designing a sgRNA is the protospacer adjacent motif (PAM) sequence on the non-targeted DNA strand. For the CRISPR Cas9 system the PAM sequence is 5'-NGG-3' where N represents any nucleotide.[16] This specific sequence drives the cleavage of the DNA by the enzyme as it occurs three to four nucleotides upstream of the PAM site. While this 5'-NGG-3' sequence should not be included in the sgRNA, it must be factored in when designing target sequences as it limits where the enzyme can bind, and the lack of a PAM sequence will disrupt efficient gene editing. To design the 17 to 20 bp oligonucleotides that will comprise the sgRNAs, there are several online tools to help filter and maximize on target efficiency while minimizing off target effects. Benchling was the online tool used for the

design of all sgRNAs in this research.

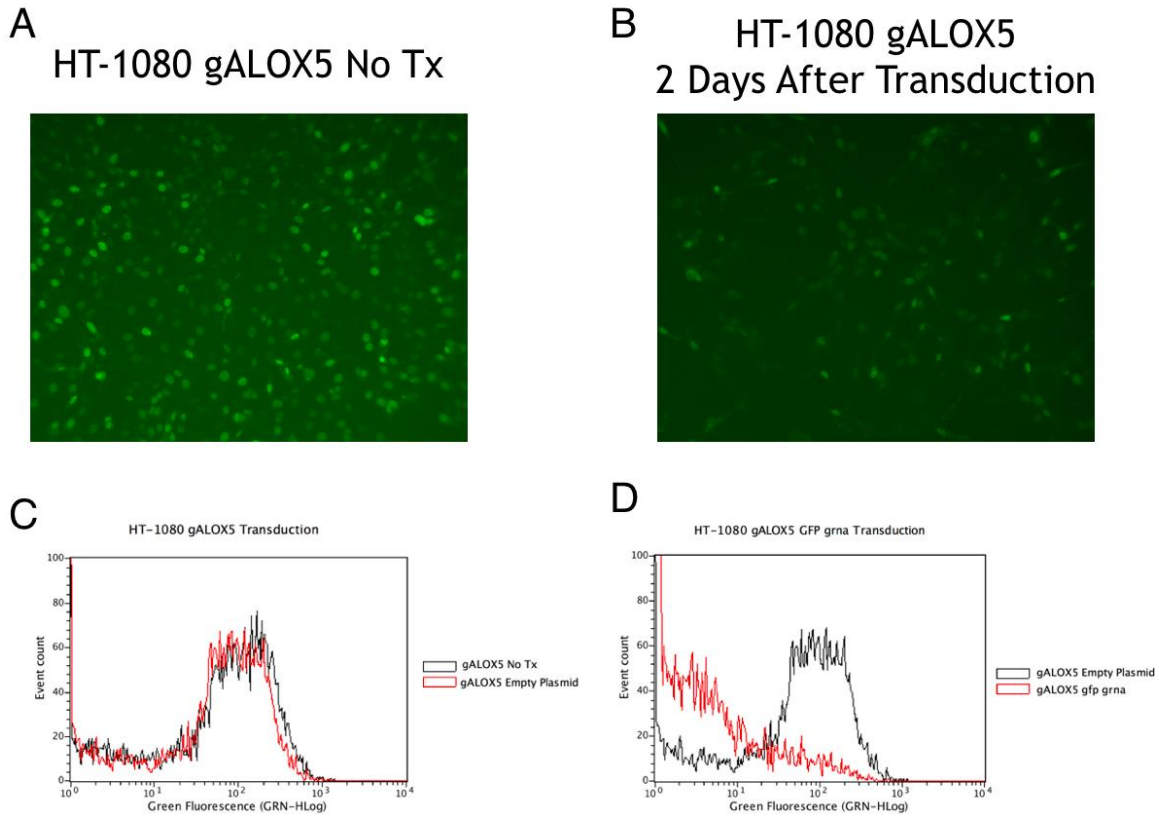

Figure 14: CRISPR knockout in HT-1080 cell line

Figure 14

CRISPR lentiviral transduction can efficiently generate knockouts in HT-1080 cells. (A) HT-1080 transduced with empty pLCV2 were designated as the non-treated cells and used as the control. These cells do not show any reduction of gfp visually. (B) Two days post transduction with pLCV2-sgGFP, HT-180 cells showed remarkable reduction of gfp expression visually. (C) Cells transduced with empty plasmid have similar gfp expression to cells that were not treated at all. This suggests pLCV2 empty is a viable control. (D)

FACs analysis quantified the reduction of gfp expression showing effective knockout of gfp in these cells via CRISPR lentiviral transduction.

After designing oligonucleotides targeting a specific gene of interest, molecular cloning methods were used to anneal oligonucleotides and ligate them into the CRISPR plasmid, lentiCRISPR v2 (pLCV2). After purification, these plasmids in conjunction with envelope plasmid pMD2.G and packaging plasmid psPAX2 were transfected into HEK-293T cells via PolyJet to induce production of lentivirus. The 48hr and 72hr viral supernatant were collected, filtered and either used or stored at -20 degrees Celsius. This viral supernatant was used to transduce the target cells to either overexpress or knock out a gene of interest. The control testing manipulated the expression of gfp in the HT-1080 and HT-1080 gALOX5 cell lines. The pLCV2 plasmid containing sgGFP was transfected into HEK-293T cells with psPAX2 and pMD2.G; 72hr later the viral supernatant was filtered and used to transduce the target cell line HT-1080 gALOX5. HT-1080 gALOX5 is a human fibrosarcoma cell line that also expresses gfp; this fluorescence can be observed visually under a fluorescence microscope and can be measured using a FACS machine. These cells were transduced with viral supernatant containing pLCV2 empty plasmid as a control as well as a viral supernatant containing the pLCV2-sgGFP. Two days post transduction of the HT-1080 gALOX5 cell line there was a significant decrease in gfp expression visually when compared to the control group (Fig. 14A, Fig. 14B). This decrease in fluorescence was confirmed with FACS (Fig. 14C, Fig. 14D). The same protocol for transfection and transduction was used to overexpress gfp using the PLCV2 plasmid with gfp CDNA. HT-1080 was the target cell line for the gfp overexpression as it

is a cell line of human fibrosarcoma that does not express gfp. For this experiment pLCV2 empty plasmid was used as a control; there was a significant increase in the expression of gfp visually in cells transduced with 1.3mL of viral supernatant when compared to cells transduced with 130uL of viral supernatant (Fig.15A, Fig. 15B). FACS analysis confirmed this increase of gfp in the HT-1080 cells (Fig. 15C). These protocols were used to create HT-1080 ACSL4 knockout stable cell lines that were blasticidin selected.

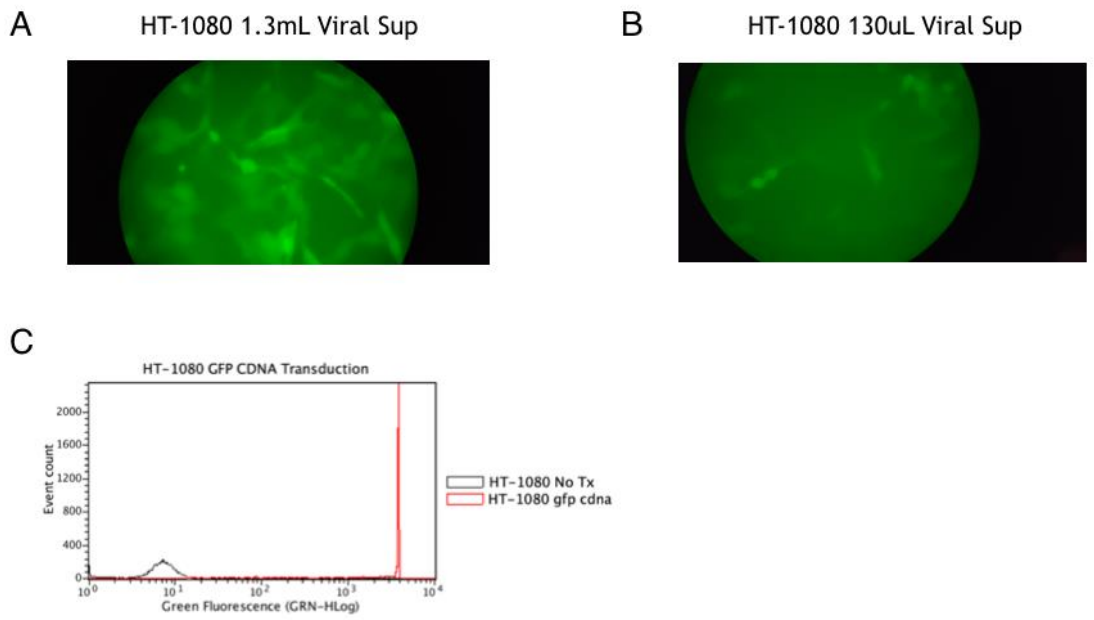

Figure 15: CRISPR is used to overexpress gfp in HT-1080

Figure 15

CRISPR lentiviral transduction can efficiently generate gfp overexpression in HT-1080 cells. (A) HT-1080 cells transduced with 1.3mL of viral sup. shows ample expression of gfp visually. (B)HT-1080 cells transduced with 130uL of viral sup. shows slight expression of gfp visually. (C) FACs analysis shows pronounced expression of gfp in cells

treated with 1.3mL of viral sup. Cells transduced with empty pLCV2 were used as the control and designated as the non-treated cells.

ACSL4 Presents as a Potential Genetic Target in Ferroptosis

These CRISPR protocols were used to create HT-1080 ACSL4 knockout stable cell lines that were blasticidin selected. Just as PPIP5K2 was a gene of interest to generate knockouts in HT-1080 and iNIL, so was Acyl-CoA Synthetase Long Chain Family Member 4 (ACSL4). There are five ACSL enzymes in mammals: among them is ACSL4, a gene involved in lipid metabolism and responsible for converting free long-chain fatty acids into fatty acyl-CoA esters.[17] As an isozyme, ACSL4 preferentially catalyzes several polyunsaturated fatty acids (PUFAs) such as arachidonic acid.[17] It is speculated that this gene is important in PUFA metabolism. The oxidation of PUFAs by lipoxygenases via a PHKG2-dependent iron pool is necessary for ferroptosis[3]. For this reason, generating an analysis of ACSL4 with CRISPR knockouts will probe for a correlation between its PUFA metabolism and PUFA oxidation in ferroptosis in MNs. Playing a role in lipid biosynthesis and fatty acid degradation, the presence of this gene has been shown in literature to drive ferroptosis. Nonetheless, the function of this gene requires further characterization and thus became a target for both iNIL and HT1080 knockouts via CRISPR lentiviral transduction.

HT-1080 cells were transduced with pLHG empty vector as well as pLHG-sgACSL4 with a specific target for exon 4 (pLHG-sgACSL4 E4). After, stable cell lines were generated via blasticidin selection and treated with erastin and RSL3 individually. HT-1080 cells not transduced with any virus were designated as no treatment (No Tx) as

well as a control for cell viability assays. HT-1080 cells transduced with empty pLHG were also used as a control for the experiment. All cells treated with erastin on the micromolar range concentration showed no difference in cell viability (Fig. 16A). On the other hand, cells treated with RSL3 on the micro molar range concentration showed that cells transduced with pLHG-sgACSL4 E4 showed a suppression of cell death (Fig. 16B). Non-transduced cells and cells transduced with empty vector displayed similar sensitivity, suggesting that the difference in sensitivity is specific to ACSL4 knockout (Fig. 16B). It should be noted that the pLHG-sgACSL4 E4 represent a polyclonal population and it is a possibility that after single clone selection a monoclonal population may give rise to further resistance to ferroptosis.

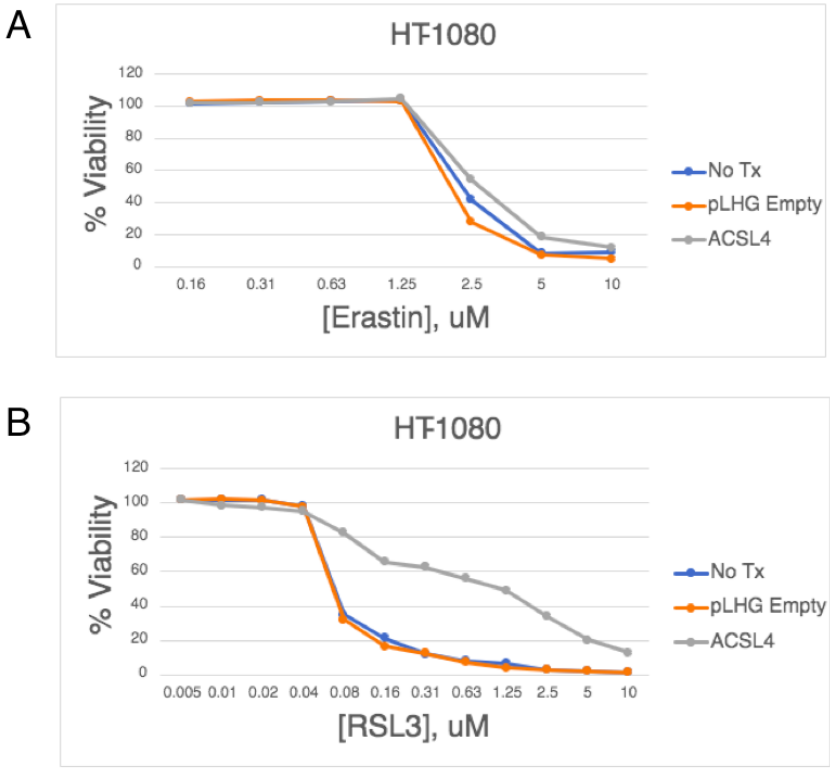

Figure 16: CRISPR knockout of ACSL4 in HT-1080 inhibits ferroptosis

Figure 16

HT-1080-sgACSL4 E4 inhibits ferroptosis induced by RSL3 (A) Erastin induces cell death in HT-1080 on the micro molar range concentration eliciting no differences in sensitivity despite ACSL4 knockout (B) RSL3 induces cell death in HT-1080 on the micro molar range concentration and is inhibited by ACSL4 knockout

---

CRISPR Knockout Optimized for Embryonic Stem Cell Stable Cell Lines

The CRISPR protocol that was effective in the HT-1080 cell line was not as effective in the iNIL embryonic stem cells. There was a slight increase in gfp expression in cells transduced with the pLCV2 gfp-CDNA plasmid, but the increase was not as

prominent as with the HT-1080 cells (Fig. 17A). As a result, the viral supernatant was concentrated using ultracentrifugation in order to deliver more virus to the embryonic stem cells. Ultracentrifugation of the virus resulted in better transduction of the iNIL cells, significantly increasing the gfp expression (Fig. 17 B). Thus, the genetic characterization of Snca, Acsl4 and Ppip5k2 in MN context can commence using this CRISPR knockout approach to develop stable cell lines lacking these genes.

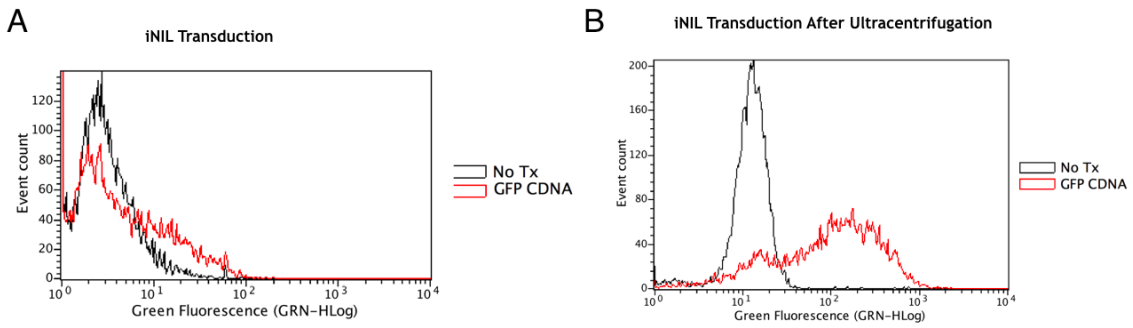

Figure 17: CRISPR is used to overexpress gfp in iNIL cells

Figure 17

iNIL cells are successfully genetically edited when transduced with concentrated virus. (A)iNIL cells are slightly transduced to express gfp following the HT-1080 protocol. (B) iNIL cells are significantly transduced to express gfp after concentrating virus via ultracentrifugation.

---

iNIL MN Ferroptosis Model Reveals Competency of ALS Drugs

While these genetic studies will require a lot of work to understand them, the benefit of having a working ferroptosis model in iNIL cells can be exploited. iNIL MNs,

where ferroptosis was induced with RSL3, were treated with three distinct ALS drugs: Riluzole, Sodium phenyl buturate (Na4PB), and Edaravone. Riluzole is a neuroprotective drug that blocks glutamatergic neurotransmission in the CNS.[18] It inhibits the release of glutamic acid from cultured neurons, from brain slices, and from corticostriatal neurons in vivo.[18] It is currently a medication used to treat patients with Amyotrophic Lateral Sclerosis (ALS). Na4PB is currently in phase 2 trials as a potential ALS treatment. Since transcription dysregulation may play a role in the pathogenesis of ALS, Sodium phenylbutyrate's mechanism of action as a histone deacetylase inhibitor is to improve transcription and post-transcriptional pathways, promoting cell survival.[19] Na4PB has shown to be effective in mouse model MNs.[19]

Finally, although the exact mechanism of action of edaravone in the treatment of ALS is unknown, its therapeutic effect may be due to its known antioxidant properties; oxidative stress is a part of the process that kills neurons in patients with ALS.[20] Given the probable involvement of ferroptosis in neurodegeneration, especially ALS it was hypothesized that one of these ALS drugs could potentially suppress cell death by ferroptosis. Ferroptosis incited in iNIL MNs by RSL3 was inhibited by only one of the three drugs, edaravone (Fig. 18). The antioxidant properties of this particular drug coincide with the putative pathway of ferroptosis.

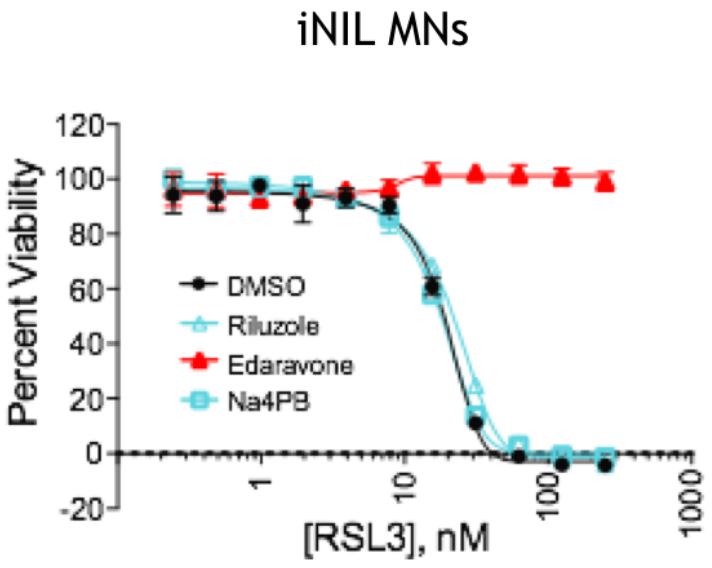

Figure 18: ALS drug edaravone inhibits ferroptosis in this MN model

Figure 18

Edaravone inhibits ferroptosis in iNIL MNs (A) Riluzole and Na4PB failed to quell cell death in iNIL MNs whereas Edaravone successfully restored cell viability.

CHAPTER 4: DISCUSSION

NSC-34 Provides a Basis for Studying Ferroptosis in a MN Context

While ferroptosis was discovered in the fibrosarcoma cell line HT-1080 and demonstrated an effective pathway to elicit in many types of cancer, its intricacies suggested it may be involved in other pathologies. This study aimed to highlight the connection, if any, that might exist between ferroptosis and motor neurons. Studying NSC-34 provided a basis for this aim since these cells were differentiated into a state that maximized its motor neuron qualities.

The first steps towards this analysis were to establish the optimal differentiation condition and the optimal drug treatment conditions. The combination of erastin, RSL3 and 50 $\mu g \cdot mL^{-1}$ ferric citrate induced ferroptosis the most effectively in NSC-34. This cell death was attributed solely to ferroptosis since PARP cleavage did not occur, an event involved in apoptosis. A signaling cascade specific to apoptosis involves the activation of cysteinyl-aspartate proteases (caspases). These caspases initiate cell death by cleaving and activating effector caspases.[21] PARP-1 is a well-known substrate of caspases and its subsequent cleavage has become an apoptosis hallmark.[21] Therefore, lack of PARP cleavage was significant in proving this cocktail elicits ferroptosis only, a non-apoptotic form of cell death. zVAD-fmk functions as a caspase inhibitor as it irreversibly binds to the catalytic site of caspase proteases to suppress apoptosis.[22] Nec-1 inhibits the kinase activity of receptor interacting protein kinase 1 (RIPK1), a key signaling effector in inducing necroptosis.[23] Both inhibitors did not suppress cell death in cells treated with FINs, but the well-known ferroptosis inhibitor fer-1 could. This is important in demonstrating the sensitization to FINs is specific to ferroptosis only.

Furthermore, a BODIPY assay was used to determine changes in lipid ROS levels in the sensitized cells. BODIPY is an oxidation sensitive fluorescent lipid peroxidation probe. It contains a long carbon chain that causes it to localize in compartments of the cell where lipid ROS would manifest. Oxidation of the polyunsaturated butadienyl portion of the dye results in a shift of the fluorescence emission peak from ~590 nm to ~510 nm, a fluorescence change that can be measured with FACS.[24] This increase in the ferroptotic hallmark lipid ROS assisted in the solidification of this cocktail as the best way to induce ferroptosis in these cells.

After the optimal differentiation condition of MEM 1% FBS without all trans retinoid acid and a three-day incubation period was determined, these cells were subject to treatment with FINs to verify and measure sensitivity differences to ferroptosis. It was discovered that differentiated cells experienced more cell death and decrease in viability when compared to its undifferentiated counterpart. The sensitivity differences between differentiated and undifferentiated cells were attributed to serum depletion in the growth media of the cells and the downregulation of the genes CTH and CBS after differentiation. Interestingly, normal cells subject to FINs and the TS Pathway inhibitor PPG were sensitized to ferroptosis similar to the response of differentiated cells. This highlighted the importance of the downregulation of Cth and Cbs in regulating differentiated cells sensitization to ferroptosis. This data revealed there may in fact be a connection between motor neurons and ferroptosis and provided a basis for this study's aim to investigate this connection. However, a cellular model that efficiently differentiated into motor neurons provided more insight.

Embryonic Stem Cells Provide a Better Model for Studying Ferroptosis Sensitivity in MNs

NSC-34 cells fluctuated in its motor neuron-like qualities depending on basal media and time frame of differentiation. Although the optimal differentiation condition in this cell line was selected to begin investigating ferroptosis in MN context, embryonic stem cells fully differentiated into motor neurons without ambiguity. This was first determined morphologically followed by a genetic analysis after probing for certain markers. Hb9 upregulation is an early event in MN differentiation; as its expression was significant in MN cultures at day 0 and day 2, this was the first indication of successful differentiation. This upregulation was quantified through FACS analysis by measuring gfp expression changes as a result of the Hb9-gfp reporter system in the embryonic stem cells. On the other hand, markers for mature motor neurons such as Chat and Tubb3 were upregulated at MN day 2 and MN day 5. Since embryonic stem cells could differentiate into motor neurons as determined both morphologically and genetically, this provided an efficient cell model to determine if there was a connection between ferroptosis and motor neurons.

Motor Neurons are Sensitized to Ferroptosis

After differentiation, the motor neurons derived from embryonic stem cells showed significant sensitivity to RSL3 treatment, resulting in cell death and a reduction in cellular viability. However, these cells were not susceptible to cell death induced by erastin, a result attributed to the lack of expression of xCT in this cell line. The sensitivity

induced by RSL3 was rescued after treatment with ferroptosis inhibitor bME. The use of bME as a ferroptosis inhibitor became of interest as a result of its use as a component in the MN media. Removing bME from the MN media made inducing ferroptosis feasible as cellular heath was not compromised and its presence would not interfere with RSL3 functionality. These findings are important in solidifying both the proper induction of ferroptosis and that the cell death is ferroptosis specific. Cell death caused by RSL3 was also suppressed by fer-1, another ferroptosis inhibitor, verifying the specificity for ferroptosis. For these reasons, it was deduced that motor neurons derived from embryonic stem cells, display ample sensitivity to ferroptosis; a significant finding since motor neuron deregulation is implicated in neurodegenerative diseases such as ALS and Alzheimer's.

Moving forward, the questions that arise include why these cells are sensitive to ferroptosis and what genes are involved in either driving or inhibiting the pathway. The first step in answering this question requires an assessment of which genes are upregulated and downregulated, leading to the IPA analysis of gene expression changes. Comparing motor neurons treated with FINs and DMSO, the software returned which pathways were involved in the genes that were upregulated and downregulated by two-fold. These biological pathways included: Synaptogenesis signaling pathway, Calcium signaling, Axonal guidance signaling, GABA receptor signaling, and Netrin signaling. Synaptogenesis is responsible for the formation of synapses; although prominent during embryogenesis, it is a process that is also involved in learning and synaptic repair.[16] The synaptogenesis signaling pathway could potentially serve as a target for novel treatment in neurodegenerative disease.[25] The fact that this pathway is also affected by ferroptosis

in the neuronal context requires further investigation. Calcium signaling mediates several processes in the cell with critical importance to neurons due to its involvement in synaptic activity and depolarizing signals.[26] It is a calcium mediated form of signal transduction with roles ranging from excitability and exocytosis to transcription and more.[26] Axonal guidance signaling involves axon guidance receptors that transmit signals to regulate precise pathfinding decisions; it has been studied as a target for axon regeneration in cells inflicted with injury or disease.[27] Moreover, GABA receptor activation inhibits the evoked release of a number of transmitters from brain tissue including: glutamate, serotonin, dopamine and GABA itself.[28] Deregulation of this pathway seems to be involved in neurological disorders. Netrin signaling involves netrins: a class of proteins associated with axon guidance; through intracellular signaling responses, netrin-1 can trigger either attraction or repulsion of the axon in response to the extracellular environment.[29]

Of these pathways returned by IPA analysis synaptogenesis signaling, calcium signaling, and netrin signaling were determined to be downregulated; while axonal guidance signaling and GABA receptor signaling were not determined. In regard to synaptogenesis signaling, this downregulation could be observed morphologically in immunostained cells treated with RSL3. There is a visible reduction of cells and formation of synapses in these cells compared to the DMSO control. With respect to calcium signaling, the downregulation of this pathway bought into question whether its involvement served as neuroprotection or to drive ferroptosis. With the use of calcium chelator EGTA to mimic calcium's down regulation we could assess this question. It was determined that EGTA treatment caused cell death and if co-treated with fer-1, this cell

death could be inhibited. These results confirmed that calcium signaling downregulation seems to drive ferroptosis. While these findings are noteworthy, there is still much to uncover in terms of how these pathways facilitate ferroptosis.

Several of the pathways that were affected by ferroptosis induction in motor neurons seem to also have a role in neurodegeneration. Further testing is required to understand in what context ferroptosis causes sensitivity in motor neurons and if there is any correlation between this sensitivity and neurodegeneration.

Why are Motor Neurons Sensitive to Ferroptosis?

In a 2012 study, adult mice were floxed by flanking exons 2 and 4 of the gpx4 gene with lox p sites.[30] These mice were crossbred with tamoxifen inducible Cre transgenic mice, enabling researchers to induce GPX4 ablation after tamoxifen treatment.[30] The study revealed that GPX4 ablation prompted lethal phenotypes including: increased mitochondrial damage, decreased activity of the electron transport chain, reduced atp production in the liver, neuronal loss in the hippocampus region and increased astrogliosis.[30] Lack of GPX4 resulted in eventual death of the mice within two weeks.[30] The data was indicative of the importance of this gene in both the survival of adult animals and neuronal health.

As we know GPX4 is a major antioxidant compromised in ferroptosis. These findings connecting GPX4 to neuronal health, as well as our findings that show direct inhibition of GPX4 with RSL3 treatment sensitizes motor neurons, illustrates the importance of ferroptosis in neuronal context. This could potentially mean the increased sensitivity is significant and warrants further investigation. If the pathway is characterized in neurons, its manipulation could lead to future novel therapies.

Nonetheless, the next step would involve a detailed study of the genes implicated in this sensitization. While RNA-seq revealed certain pathways that may be of interest, the stable cell lines with CRISPR knockouts provide the means to manipulate and study individual genes in diverse contexts.

The Importance of Genetic Studies in Understanding Ferroptosis in Future Experiments

Lack of PPIP5K2 expression via siRNA treatment proved to serve as an inhibitor of ferroptosis as it rescued cell death when cells were treated with erastin or RSL3. This data suggests that the PPIP5K2 gene is important in driving ferroptosis. Creating stable cell lines with PPIP5K2 knockouts will help detail this gene's involvement in driving ferroptosis, as well as more information regarding its potential as a therapeutic target where ferroptosis is prominent.

ACSL4 is another gene that appears to drive ferroptosis as it is responsible for the formation of PUFAs. PUFA formation in ferroptosis is imperative as it forms lipid peroxides in the presence of iron via esterification and oxygenation[3]. It is one of the speculated routes that iron takes advantage of to induce cell death. Therefore, inhibiting this gene could rescue cell death and CRISPR knockouts can characterize to what extent this gene is involved in ferroptosis. Moreover, Snca revealed as the upstream regulator of downregulated genes in the iNIL MN model is yet another target to investigate. PPIP5K2, ACSL4 and Snca are not the only genes implicated in the ferroptotic pathway, thus the CRISPR knockouts provide a means to detail this pathway and filter which genes are of the most importance. These genetic studies are essential because they not only

provide insight on the mechanisms at play when ferroptosis is induced but they also provide effective targets.

iNIL Cells Differentiated into MNs Provide a Viable Model to Screen ALS Drugs and Find Potential Therapeutic Targets for Neurodegenerative Pathologies

The inhibition of ferroptosis by ALS drug edaravone fortifies that this MN model is not only effective at delineating ferroptosis in MNs but provides a basis to screen ALS drugs. Additionally, this model can be used to identify potential therapies in any pathological context depicted by neurodegeneration, especially if compromised potentially with ferroptosis involvement. The data here shows the versatility of the iNIL MN model and the prospective work that can be achieved with its use.

Overall, the research in this study supports the main aim to establish a connection between ferroptosis and motor neurons providing the groundwork to delve into the following: using the iNIL MN model to investigate neurodegeneration, analyzing pertinent genetic studies using iNIL for characterization in MNs and HT-1080 for in depth characterization of ferroptosis itself.

To recapitulate, NSC-34 provided the initial model to investigate ferroptosis in MNs but as a result of extrinsic factors that caused sensitivity changes, iNIL provided a more suitable model. In this process, several genes were highlighted as targets for depicting this cell death modality in MNs. In addition to uncovering ferroptosis' mechanism of action, another fundamental feature of the iNIL MN model is its ability to investigate the intricacies of neurological pathologies.

REFERENCES

1. *Li J, Cao F, Yin H-liang, Huang Z-jian, Lin Z-tao, Mao N, Sun B, Wang G. Ferroptosis: past, present and future. Nature News. 2020 Feb 3 [accessed 2020 Mar 16]. https://www.nature.com/articles/s41419-020-2298-2*

2. *Lei P, Bai T, Sun Y. Mechanisms of Ferroptosis and Relations With Regulated Cell Death: A Review. Frontiers in physiology. 2019 Feb 26 [accessed 2020 Mar 16]. https://www.ncbi.nlm.nih.gov/pmc/articles/PMC6399426/*

3. *Yang WS, Kim KJ, Gaschler MM, Patel M, Shchepinov MS, Stockwell BR. Peroxidation of polyunsaturated fatty acids by lipoxygenases drives ferroptosis. Proceedings of the National Academy of Sciences of the United States of America. 2016 Aug 9 [accessed 2020 Mar 16]. https://pubmed.ncbi.nlm.nih.gov/27506793/*

4. *Dolma S, Lessnick SL, Hahn WC, Stockwell BR. Identification of genotype-selective antitumor agents using synthetic lethal chemical screening in engineered human tumor cells. Cancer cell. 2003 Mar 3 [accessed 2020 Mar 16]. https://pubmed.ncbi.nlm.nih.gov/12676586/*

5. *Yang WS, Stockwell BR. Synthetic lethal screening identifies compounds activating iron-dependent, nonapoptotic cell death in oncogenic-RAS-harboring cancer cells. Chemistry & biology. 2008 Mar [accessed 2020 Mar 16]. https://www.ncbi.nlm.nih.gov/pmc/articles/PMC2683762/*

6. *Yang WS, Stockwell BR. Ferroptosis: Death by Lipid Peroxidation. Trends in cell biology. 2016 Mar [accessed 2020 Mar 16]. https://www.ncbi.nlm.nih.gov/pmc/articles/PMC4764384/*

7. *Cashman NR, Durham HD, Blusztajn JK, Oda K, Tabira T, Shaw IT, Dahrouge S, Antel JP. Neuroblastoma x spinal cord (NSC) hybrid cell lines resemble developing motor neurons. Developmental dynamics : an official publication of the American Association of Anatomists. 1992 Jul [accessed 2020 Mar 16]. https://pubmed.ncbi.nlm.nih.gov/1467557/*

8. *Madji Hounoum B, Vourc'h P, Felix R, Corcia P, Patin F, Guéguinou M, Potier-Cartereau M, Vandier C, Raoul C, Andres CR, et al. NSC-34 Motor Neuron-Like Cells Are Unsuitable as Experimental Model for Glutamate-Mediated Excitotoxicity. Frontiers in cellular neuroscience. 2016 May 9 [accessed 2020 Mar 17]. https://www.ncbi.nlm.nih.gov/pmc/articles/PMC4860417/#:~:text=NSC%2D34%20is%20an%20hybrid,protocols%20of%20differentiation%20and%20maturation.*

9. *Mazzoni EO, Mahony S, Closser M, Morrison CA, Nedelec S, Williams DJ, An D, Gifford DK, Wichterle H. Synergistic binding of transcription factors to cell-*

specific enhancers programs motor neuron identity. Nature News. 2013 Jul 21 [accessed 2020 Mar 17]. https://www.nature.com/articles/nn.3467

10. *Arber S, Han B, Mendelsohn M, Smith M, Jessell TM, Sockanathan S. Requirement for the Homeobox Gene Hb9 in the Consolidation of Motor Neuron Identity. Neuron. 2001 Jun 12 [accessed 2020 Mar 16]. https://www.sciencedirect.com/science/article/pii/S089662730180026X*

11. *Coufal N. Notes of markers for neural differentiation.2009 [accessed 2020 Mar 16]. https://commonfund.nih.gov/sites/default/files/Differentiation_NSC.pdf*

12. Tanapat P. Neuronal Cell Markers. Materials and Methods. 2021 Mar 10 [accessed 2021 Mar 16]. https://www.labome.com/method/Neuronal-Cell-Markers.html

13. Kapitein LC, Hoogenraad CC. Building the Neuronal Microtubule Cytoskeleton. Neuron. 2015 Aug 5 [accessed 2020 Mar 16]. https://pubmed.ncbi.nlm.nih.gov/26247859/

14. *Weaver JD, Wang H, Shears SB. The kinetic properties of a human PPIP5K reveal that its kinase activities are protected against the consequences of a deteriorating cellular bioenergetic environment. Bioscience reports. 2013 Feb 5 [accessed 2020 Mar 16]. https://pubmed.ncbi.nlm.nih.gov/23240582/*

15. *PPIP5K2 Gene (Protein Coding). GeneCards. [accessed 2020 Mar 16]. https://www.genecards.org/cgi-bin/carddisp.pl?gene=PPIP5K2*

16. *Full Stack Genome Engineering. Synthego. [accessed 2020 Mar 16]. https://www.synthego.com/guide/how-to-use-crispr/sgrna*

17. *Kuwata H, Hara S. Role of acyl-CoA synthetase ACSL4 in arachidonic acid metabolism. Prostaglandins & other lipid mediators. 2019 Jul 12 [accessed 2020 Mar 16]. https://pubmed.ncbi.nlm.nih.gov/31306767/*

18. *Doble A. The pharmacology and mechanism of action of riluzole. Neurology. 1996 Dec [accessed 2020 Mar 17]. https://pubmed.ncbi.nlm.nih.gov/8959995/#:~:text=Riluzole%20is%20a%20neuroprotective%20drug%20that%20blocks%20glutamatergic%20neurotransmission%20in%20the%20CNS.&text=In%20vitro%2C%20riluzole%20protects%20cultured,patients%20with%20amyotrophic%20lateral%20sclerosis.*

19. *Cudkowicz ME, Andres PL, Macdonald SA, Bedlack RS, Choudry R, Brown Jr RH, Zhang H, Schoenfeld DA, Shefner J, Matson S, et al. Phase 2 study of sodium phenylbutyrate in ALS. Amyotrophic lateral sclerosis : official publication of the World Federation of Neurology Research Group on Motor Neuron Diseases. 2009 Apr [accessed 2020 Mar 17]. https://pubmed.ncbi.nlm.nih.gov/18688762/*

20. *Cho HE, Shukla S. Role of Edaravone as a Treatment Option for Patients with Amyotrophic Lateral Sclerosis. Pharmaceuticals (Basel, Switzerland). 2020 Dec 31 [accessed 2020 Mar 17]. https://www.ncbi.nlm.nih.gov/pmc/articles/PMC7823603/*

21. *Chaitanya GV, Steven AJ, Babu PP. PARP-1 cleavage fragments: signatures of cell-death proteases in neurodegeneration. Cell communication and signaling : CCS. 2010 Dec 22 [accessed 2020 Mar 16]. https://www.ncbi.nlm.nih.gov/pmc/articles/PMC3022541/*

22. *Pan-Caspase inhibitor - Z-VAD-FMK. InvivoGen. 2021 Mar 7 [accessed 2021 Mar 16]. https://www.invivogen.com/z-vad-fmk*

23. *Takahashi N, Duprez L, Grootjans S, Cauwels A, Nerinckx W, DuHadaway JB, Goossens V, Roelandt R, Van Hauwermeiren F, Libert C, et al. Necrostatin-1 analogues: critical issues on the specificity, activity and in vivo use in experimental disease models. Cell death & disease. 2012 Nov 29 [accessed 2020 Mar 16]. https://www.ncbi.nlm.nih.gov/pmc/articles/PMC3542611/*

24. *BODIPY™ 581/591 C11 (Lipid Peroxidation Sensor). Thermo Fisher Scientific - US. [accessed 2020 Mar 16]. https://www.thermofisher.com/order/catalog/product/D3861#/D3861*

25. *Nelson TJ, Alkon DL. Molecular regulation of synaptogenesis during associative learning and memory. Brain Research. 2014 Dec 5 [accessed 2020 Mar 16]. https://www.sciencedirect.com/science/article/abs/pii/S0006899314016606#:~:text=Synaptogenesis%20plays%20a%20central%20role%20in%20associative%20learning%20and%20memory.&text=Cell%E2%80%93cell%20contact%20and%20soluble,astrocytes%20are%20important%20in%20synaptogenesis.&text=Intracellular%20signaling%20pathways%20involving%20protein,is%20required%20for%20associative%20memory.*

26. *Clapham DE. Calcium signaling. Cell. 2007 Dec 14 [accessed 2020 Mar 16]. https://pubmed.ncbi.nlm.nih.gov/18083096/*

27. *Bashaw GJ, Klein R. Signaling from axon guidance receptors. Cold Spring Harbor perspectives in biology. 2010 May [accessed 2020 Mar 16]. https://www.ncbi.nlm.nih.gov/pmc/articles/PMC2857166/*

28. *Enna SJ. GABAB Receptor Signaling Pathways. 2001[accessed 2020 Mar* 16*]https://link.springer.com/chapter/10.1007/978-3-642-56833-6_13*

29. *Boyer NP, Gupton SL. Revisiting Netrin-1: One Who* Guides *(Axons). Frontiers in cellular neuroscience. 2018 Jul 31 [accessed 2020 Mar 16]. https://www.ncbi.nlm.nih.gov/pmc/articles/PMC6080411/*

30. *Yoo S-E, Chen L, Na R, Liu Y, Rios C, Van Remmen H, Richardson A, Ran Q. Gpx4 ablation in adult mice results in a lethal phenotype accompanied by neuronal loss in brain. Free radical biology & medicine. 2012 May 1 [accessed 2020 Mar 16]. https://www.ncbi.nlm.nih.gov/pmc/articles/PMC3341497/*

Vita

Name	*Alejandra Martinez*
Baccalaureate Degree	*Bachelor of Science/Arts*, *St. Joseph's College, Brooklyn Major: Biology*
Date Graduated	*May, 2014*
Other Degrees and Certificates	*Master of Science, St. John's University, Queens, Major: Biology*
Date Graduated	*Spring, 2017*